Lecture Series Buenos Aires

18-3-2024 until 22-3-2024

Lecture F5 – Nonlinear pulse compression

Federico Furch

furch@mbi-berlin.de

Max-Born-Institut

Nonlinear Pulse Post-compression

A state-of-the-art laser system for attosecond science: an alternative

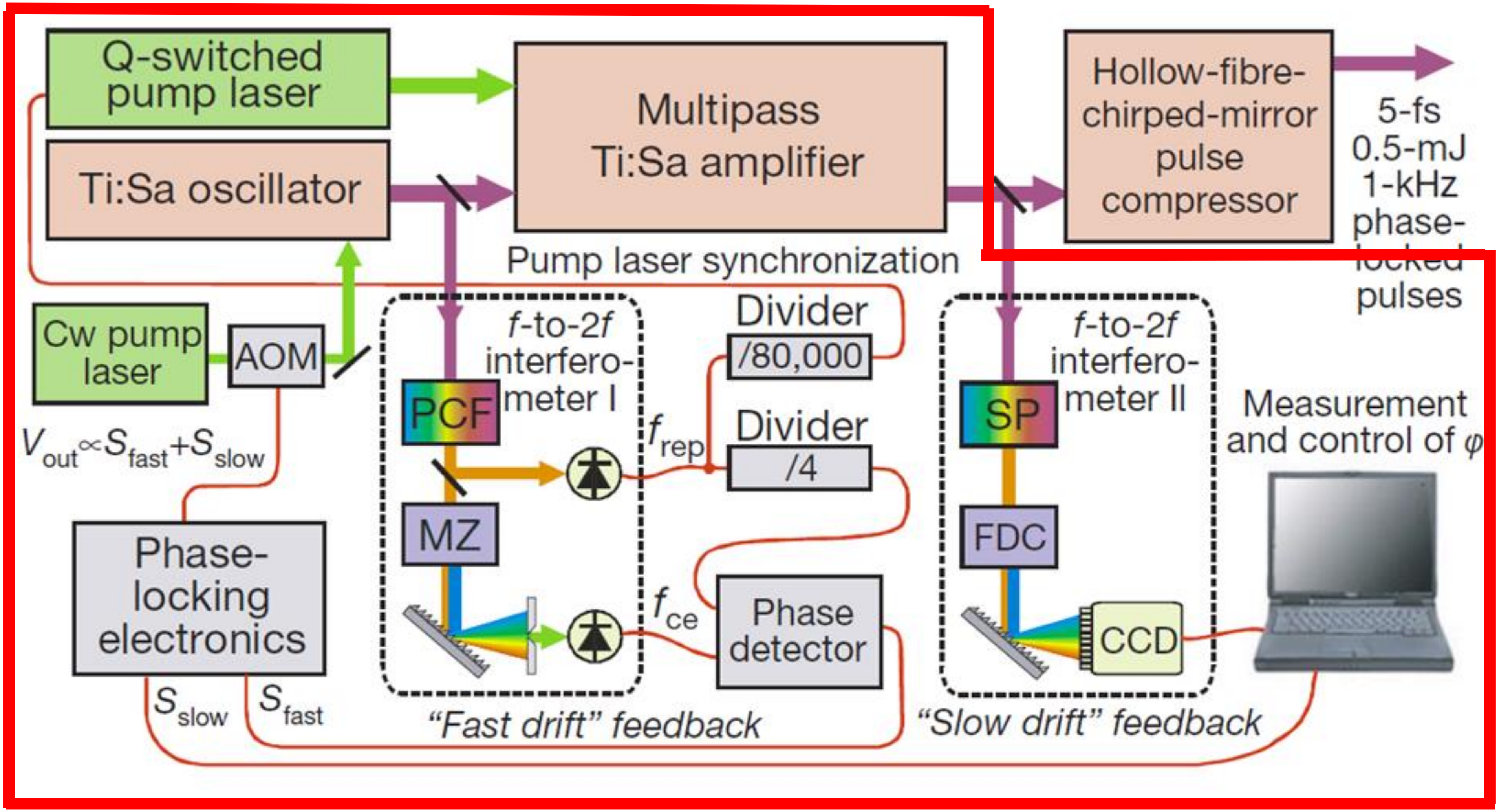

A. Baltuska et al., Nature 421, 611 (2003)

Limitations of Ti:Sapphire CPAs

Limitations to spectral range

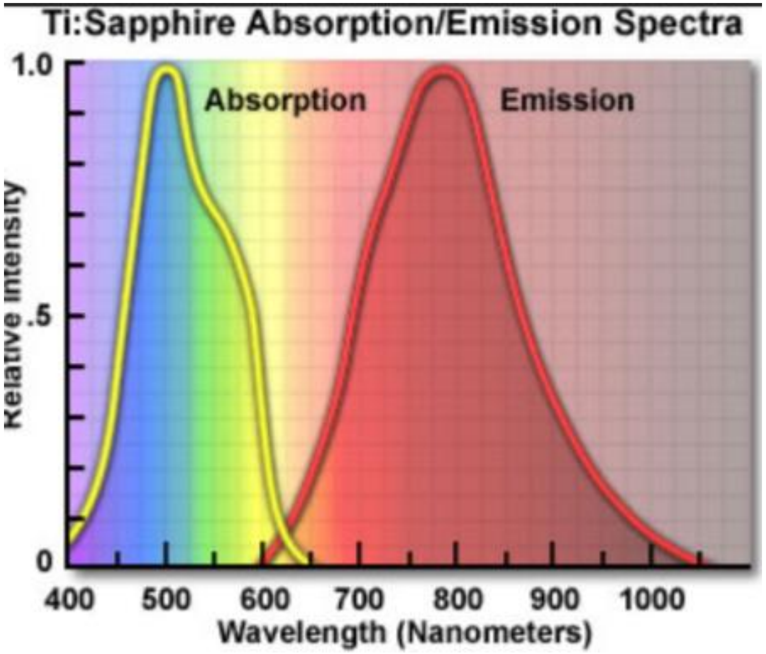

e.g. we want longer wavelength for cut-off extension during HHG

Limitations of Ti:Sapphire CPAs

Limitations to spectral range

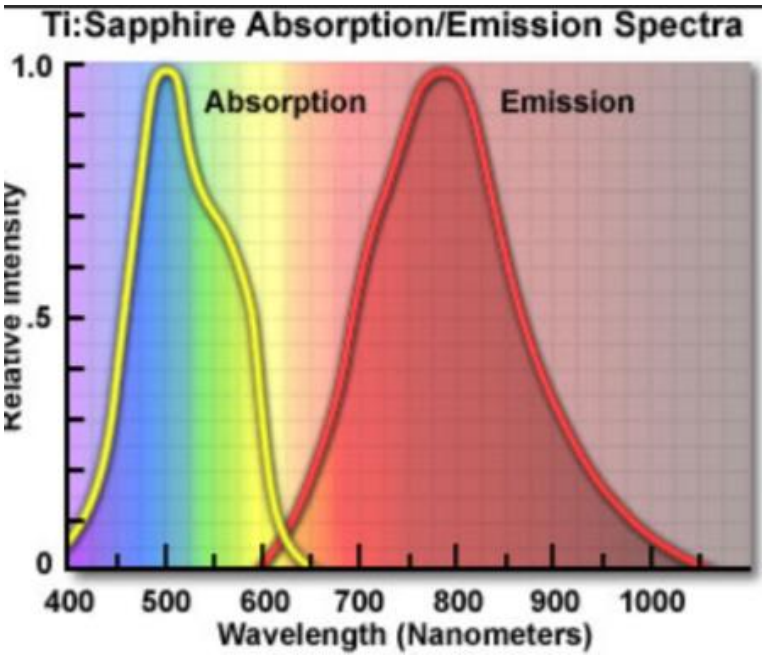

Limitations to pulse duration

gain $\sim e^{g(\omega)L}$

gain narrowing $\Delta\omega_{out} \ll \Delta\omega_{g(\omega)}$

Nonlinear pulse post-compression necessary to reach few-cycle pulse durations

Limitations of Ti:Sapphire CPAs

Limitations to spectral range

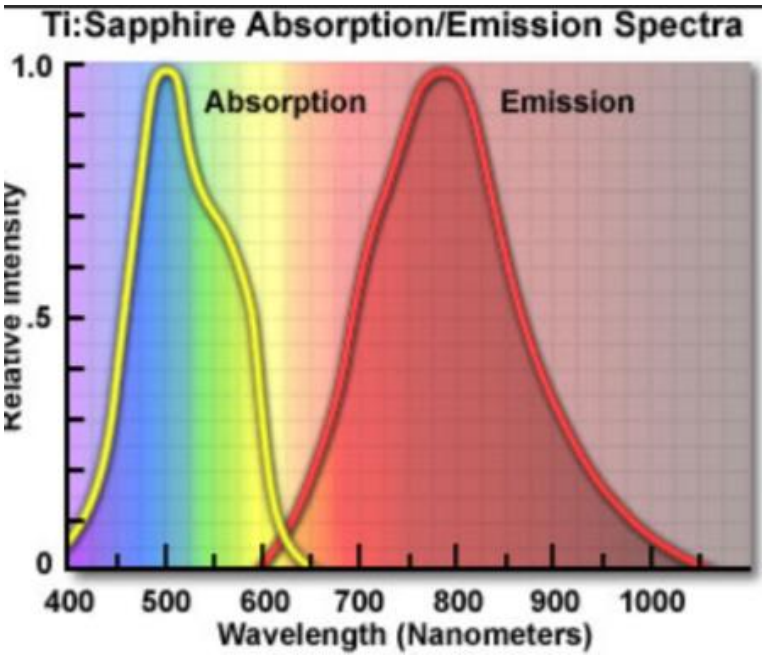

Limitations to pulse duration

gain $\sim e^{g(\omega)L}$

gain narrowing $\Delta\omega_{out} \ll \Delta\omega_{g(\omega)}$

Limitations to power scaling

$$P_{avg} = Energy_{pulse} * f_{rep.rate}$$

Fraction of pump that turns into heat $1 - \frac{\hbar\omega_{laser}}{\hbar\omega_{pump}}$

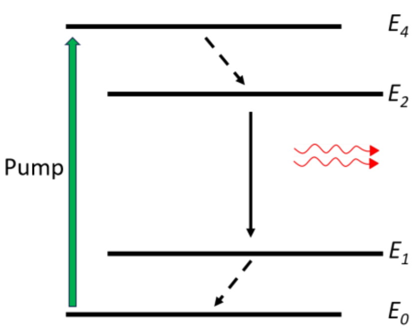

Limitations of Ti:Sapphire CPAs

Limitations to spectral range

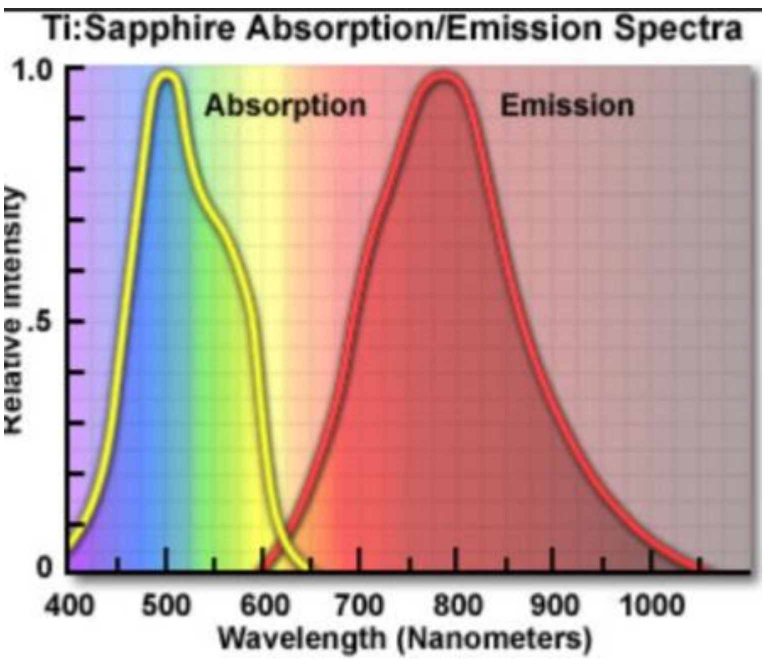

$$P_{pump}(x,y) \propto e^{-2(x^2+y^2)/w^2}$$

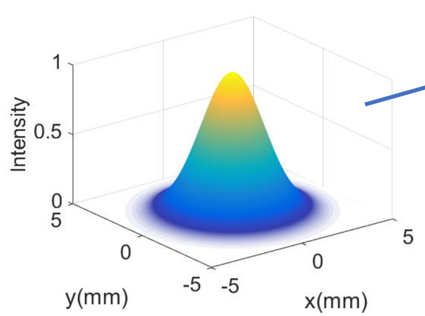

Limitations to pulse duration

gain $\sim e^{g(\omega)L}$

gain narrowing $\Delta\omega_{out} \ll \Delta\omega_{g(\omega)}$

Limitations to power scaling

$$P_{avg} = Energy_{pulse} * f_{rep.rate}$$

Fraction of pump that turns into heat $1 - \frac{\hbar\omega_{laser}}{\hbar\omega_{pump}}$

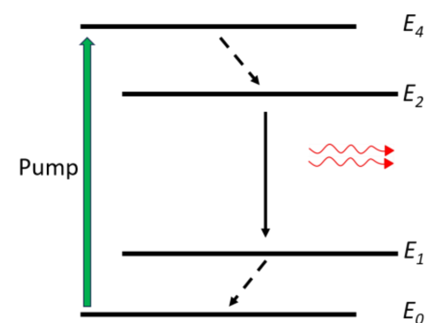

Heat source profile: may originate

- Thermal lensing (dn/dT)
- Thermal induced birefringence
- Damage of material

A laser material for high average power

Yb-doped Yttrium
Aluminum Garnet
Yb:YAG

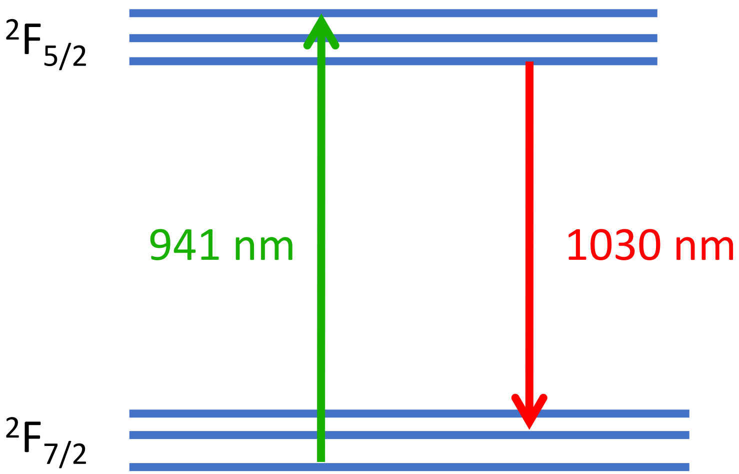

- Absorption band at InGaAs wavelengths
  - High power laser diodes are commercially available
- Low quantum defect ($1 - \frac{\hbar\omega_{laser}}{\hbar\omega_{pump}} < 0.1$)
  - Potential for high average power operation
- Long upper level lifetime (~1 msec)
  - Efficiently store energy from low peak power pump
- High quality (large) crystals
  - Crystalline or ceramic form
- BUT narrow gain bandwidth: post-compression, OPCPAs

Alternatives using Yb systems

Ti:Sapphire → ultrashort pulses
Yb-doped → high energy, high average power

Energy transfer in Optical Parametric Amplifier

Yb-doped → high energy, high average power
Nonlinear pulse compression with large compression factors to reach sub-50 fs and even sub-10 fs pulses

Nonlinear pulse compression

Third order nonlinear process $|P| \propto \chi^{(3)}|E|^3$

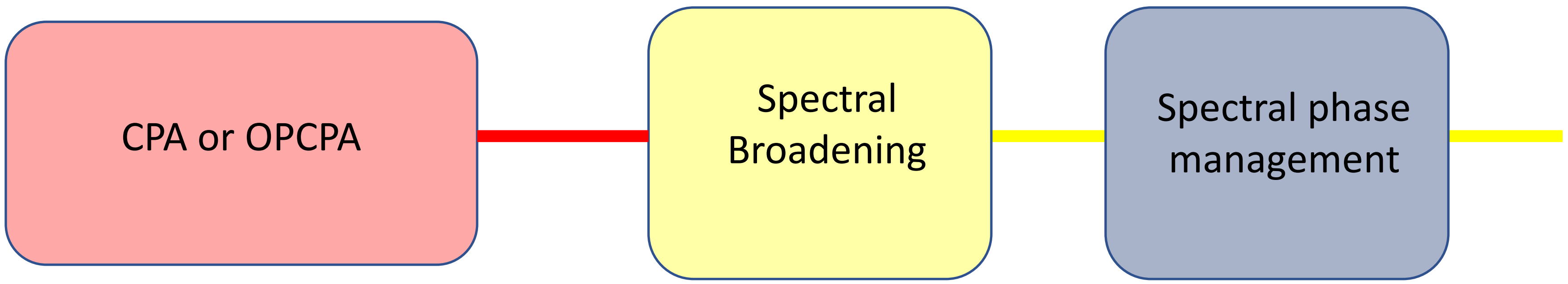

- Spectral broadening of laser pulses during nonlinear interaction of intense light pulses with a material
- Spectral phase “flattening” (dispersion compensation): usually with dispersive mirrors

Propagation equations

More details on Couairon et al., “Practitioner’s guide to laser pulse propagation models and simulations,” Eur. Phys. Journal **199**, 5-76 (2011).

$$\nabla \times \mathbf{E} = -\frac{\partial \mathbf{B}}{\partial t}$$

$$\nabla \times \mathbf{B} = \mu_0 \left(\mathbf{J} + \frac{\partial \mathbf{D}}{\partial t} \right)$$

$$\hat{\mathbf{D}}(\mathbf{r}, \omega, z) = \epsilon_0 \epsilon(\omega) \hat{\mathbf{E}}(\mathbf{r}, \omega, z) + \hat{\mathbf{P}}(\mathbf{r}, \omega, z),$$

The polarization vector models the electronic response of the medium to the electric field of the laser. Can be written as a linear and a nonlinear part: $\mathbf{P} = \mathbf{P}^{(1)}$ **and** $\mathbf{P}^{(NL)}$**.**

$$\hat{\mathbf{P}}^{(1)}(\mathbf{r}, \omega, z) = \epsilon_0 \chi^{(1)}(\omega) \hat{\mathbf{E}}(\mathbf{r}, \omega, z),$$

$$\text{where } \epsilon(\omega) \equiv 1 + \chi^{(1)}(\omega)$$

$\epsilon(\omega) = n(\omega)^2$ Permittivity.

Susceptibility χ is a tensor.

Propagation equations

$$\nabla^2\mathbf{E} - \nabla(\nabla\cdot\mathbf{E}) - \frac{1}{c^2}\frac{\partial^2}{\partial t^2}\int_{-\infty}^{t}\epsilon(t-t')\mathbf{E}(\mathbf{r},t',z)dt' = \mu_0\left(\frac{\partial\mathbf{J}}{\partial t} + \frac{\partial^2\mathbf{P}}{\partial t^2}\right)$$

With P = $P^{(NL)}$. We now move to the frequency domain

$$\nabla^2\hat{\mathbf{E}} - \nabla(\nabla\cdot\hat{\mathbf{E}}) + \frac{\omega^2 n^2(\omega)}{c^2}\hat{\mathbf{E}} = \mu_0\left(-i\omega\hat{\mathbf{J}} - \omega^2\hat{\mathbf{P}}\right)$$

Field oscillates perpendicular to **k** // **z**

Reasonable if not tightly focused (low numerical apertures)

As before, we assume $\vec{E} = E\hat{x}$

$$(\partial_z^2 + \nabla_\perp^2)E(\mathbf{r},t,z) - \frac{1}{c^2}\frac{\partial^2}{\partial t^2}\int_{-\infty}^{t}\epsilon(t-t')\mathrm{E}(\mathbf{r},t',z)dt' = \mu_0\left(\frac{\partial^2 P}{\partial t^2} + \frac{\partial J}{\partial t}\right)$$

We include J en $P^{(NL)}$ identifying: $J(\mathbf{r},t,z) \leftrightarrow \partial_t P(\mathbf{r},t,z)$

$$\hat{J}(\mathbf{r},\omega,z) \leftrightarrow -i\omega\hat{P}(\mathbf{r},\omega,z)$$

Propagation equations

$$(\partial_z^2 + \nabla_\perp^2)E(\mathbf{r},t,z) - \frac{1}{c^2}\partial_t^2 \int_{-\infty}^{t} n^2(\mathbf{r},t-t',z)E(\mathbf{r},t',z)\,dt' = \mu_0 \partial_t^2 P(\mathbf{r},t,z)$$

$$(\partial_z^2 + \nabla_\perp^2)\hat{E}(\mathbf{r},\omega,z) + k^2(\omega)\hat{E}(\mathbf{r},\omega,z) = -\mu_0\omega^2\hat{P}(\mathbf{r},\omega,z)$$

$$k(\omega) \equiv n(\omega)\omega/c.$$

Next step is to factorize the first term and separate forward and backward propagation

$$(\partial_z + ik(\omega))\,(\partial_z - ik(\omega))\,\hat{E} = -\Delta_\perp \hat{E} - \mu_0\omega^2\hat{P}(\mathbf{r},\omega,z)$$

Ignoring diffraction and NL response ...

$$\hat{E}(\omega,z) = \hat{A}_+(\omega)\exp[ik(\omega)z] + \hat{A}_-(\omega)\exp[-ik(\omega)z]$$

Forward propagation: $|\hat{A}_-| \ll |\hat{A}_+|$ $\quad \partial_z + ik(\omega) \simeq 2ik(\omega)$

Forward Maxwell Equation

$$\frac{\partial \hat{E}}{\partial z} = ik(\omega)\hat{E} + \frac{i}{2k(\omega)}\Delta_\perp \hat{E} + \frac{i}{2n(\omega)}\frac{\omega}{c}\frac{\hat{P}}{\epsilon_0}$$

Valid equation for beams with low numerical aperture

Still very general equation: all the nonlinear interactions included in *P*

Moving frame of reference

For practical purposes (i.e. numerical simulations) we change to a frame of reference moving with the pulse (at the group velocity) ulso

$$(z,t) \rightarrow (\zeta,\tau)$$

$$\zeta = z, \qquad \tau = t - z/v_g$$

$$\partial_z = \partial_\zeta - (1/v_g)\partial_\tau, \qquad \partial_t = \partial_\tau$$

$$\text{i.e. } \partial_z = \partial_\zeta + i(\omega/v_g)$$

$$\boxed{\frac{\partial \hat{E}}{\partial \zeta} = i[k(\omega) - \omega/v_g]\hat{E} + \frac{i}{2k(\omega)}\Delta_\perp \hat{E} + \frac{i}{2n(\omega)}\frac{\omega}{c}\frac{\hat{P}}{\epsilon_0}}$$

Dispersion

Center of pulse at τ=0

Difraction

Nonlinear response

Envelope equation

Computationally less expensive

$$E(\mathbf{r},\tau,\zeta) = \mathcal{E}(\mathbf{r},\tau,\zeta)\exp[i(k_0 - \omega_0/v_g)\zeta - i\omega_0\tau]$$

We assume that the source terms have a similar decomposition

$$\{P,J\}(\mathbf{r},\tau,\zeta) = \{\mathcal{P},\mathcal{J}\}(\mathbf{r},\zeta,\tau)\exp[i(k_0 - \omega_0/v_g)\zeta - i\omega_0\tau]$$

And we get the genral equation in the frequency domain:

$$\boxed{\frac{\partial\tilde{\mathcal{E}}}{\partial\zeta} = i\mathcal{K}(\Omega,\mathbf{k}_\perp)\tilde{\mathcal{E}} + i\mathcal{Q}(\Omega,\mathbf{k}_\perp)\frac{\tilde{\mathcal{P}}}{2\epsilon_0}}$$

$$\Omega \equiv \omega - \omega_0$$

$$\mathcal{K}(\Omega,\mathbf{k}_\perp) = k(\omega) - \kappa(\omega) - \frac{ck_\perp^2}{2n_0\omega} \qquad \kappa(\omega) \equiv k_0 + (\omega - \omega_0)/v_g$$

$$\mathcal{Q}(\Omega,\mathbf{k}_\perp) = \frac{\omega}{cn_0}$$

Third-order effects

Assume centro-symmetric material and no ionization ($J = 0, \chi^{(2)} = 0$)

$$\mathbf{P} \equiv \epsilon_0 \chi^{(3)} \mathbf{E}^3$$

$$E = \frac{1}{2}[\mathcal{E} \exp(ik_0 z - i\omega_0 t) + \mathcal{E}^* \exp(-ik_0 z + i\omega_0 t)]$$

$$E^3 = \frac{1}{8}[\mathcal{E}^3 \exp(i3k_0 z - i3\omega_0 t) + 3|\mathcal{E}|^2 \mathcal{E} \exp(ik_0 z - i\omega_0 t) + \mathrm{c.c.}]$$

Ignore third-harmonic (no phase matching)

$$P = \frac{1}{2}[\mathcal{P} \exp(ik_0 z - i\omega_0 t) + \mathcal{P}^* \exp(-ik_0 z + i\omega_0 t)]$$

$$\mathcal{P} \equiv \epsilon_0 \chi^{(3)} \frac{3}{4} |\mathcal{E}|^2 \mathcal{E}$$

Using the definitions of intensity and nonlinear index of refraction:

$$n_2 \equiv 3\chi^{(3)} / 4\epsilon_0 c n_0^2 \qquad \mathcal{I} \equiv \epsilon_0 c n_0 |\mathcal{E}|^2 / 2$$

$$\boxed{\frac{\mathcal{P}}{\epsilon_0} \equiv 2 n_0 n_2 \mathcal{I} \mathcal{E}}$$

Third-order effects

$$\frac{\partial \tilde{\varepsilon}}{\partial z} = i\left[k(\omega) - k_0 - \frac{(\omega - \omega_0)}{v_g} - c\,\frac{(k_x^2 + k_x^2)}{2n_0\omega}\right]\tilde{\varepsilon} + i\,\frac{\omega}{cn_0}\frac{\tilde{\mathcal{P}}}{2\epsilon_0}$$

Dispersion

Center of
pulse at τ=0

Difraction

Nonlinear
response (Fourier
Transform of *P*)

Third-order effects

$$\frac{\partial \tilde{\varepsilon}}{\partial z} = i \cancel{\left[k(\omega) - k_0 - \frac{(\omega - \omega_0)}{v_g} - c\,\frac{(k_x^2 + k_x^2)}{2 n_0 \omega} \right]} \tilde{\varepsilon} + i \frac{\omega}{c n_0} \frac{\tilde{\mathcal{P}}}{2 \epsilon_0}$$

Inverse Fourier Transform to obtain equation in the temporal domain

$$\tilde{\mathcal{P}} = \int_{-\infty}^{+\infty} \mathcal{P}(t) e^{i\Omega t} dt \qquad \frac{\mathcal{P}(t)}{\epsilon_0} = 2 n_0 n_2 \varepsilon(t) I(t)$$

$$\frac{\partial \tilde{\varepsilon}}{\partial z} = i \frac{(\omega_o + \Omega)}{c n_0} FT[n_0 n_2 \varepsilon(t) I(t)] = i \frac{\omega_0 n_2}{c} FT[\varepsilon(t) I(t)] + i \frac{n_2}{c} FT^{-1}[\Omega FT[\varepsilon(t) I(t)]]$$

Using properties of Fourier Transform: $i\Omega FT[f(t)] = FT\left[\frac{\partial f}{\partial t}\right]$

$$\boxed{\frac{\partial \varepsilon}{\partial z} = i \frac{\omega_0 n_2}{c} I \varepsilon + \frac{n_2}{c} \frac{\partial (I\varepsilon)}{\partial t}}$$

Kerr effect

Self-steepening

Kerr effect: self-phase modulation (SPM)

$$\frac{\partial \varepsilon}{\partial z} = i\frac{\omega_0 n_2}{c} I\varepsilon \Rightarrow \varepsilon = \varepsilon_0 e^{i\frac{\omega_0 n_2}{c} Iz}$$

Phase modulation in time, with instantaneous frequency generating an approximately linear chirp in the center of the pulse

$$\omega(t) = \frac{d\phi(t)}{dt}$$
$$= \omega_0 - \frac{\omega_0}{c} n_2 z \frac{dI(t)}{dt}$$

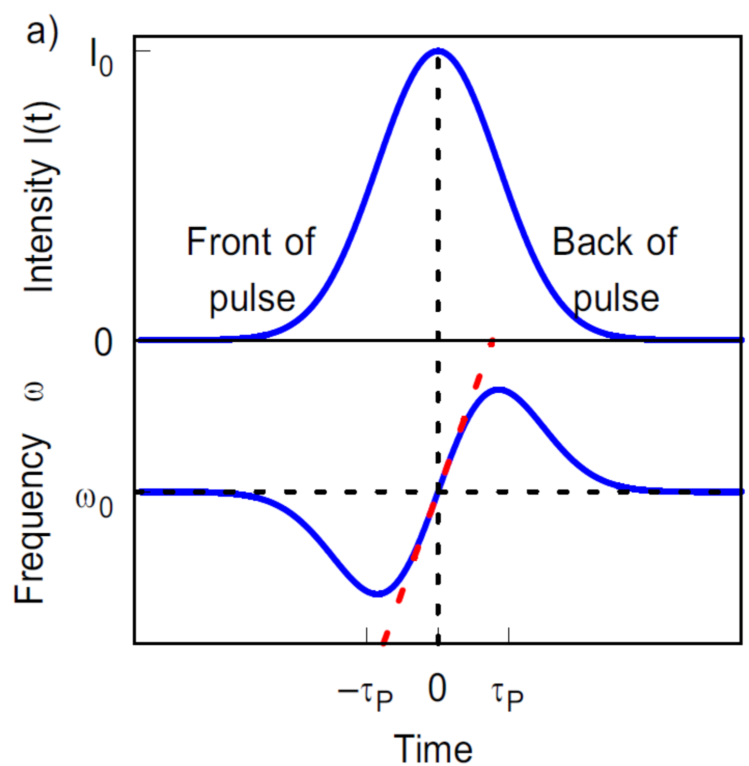

Adapted from M. Galbraith, doctoral thesis, FU-Berlin and MBI 2017

Kerr effect: self-phase modulation (SPM)

$$\varepsilon = e^{i\frac{\omega_0 n_2}{c} I z}$$

Spectrally SPM induces spectral broadening and spectral modulation

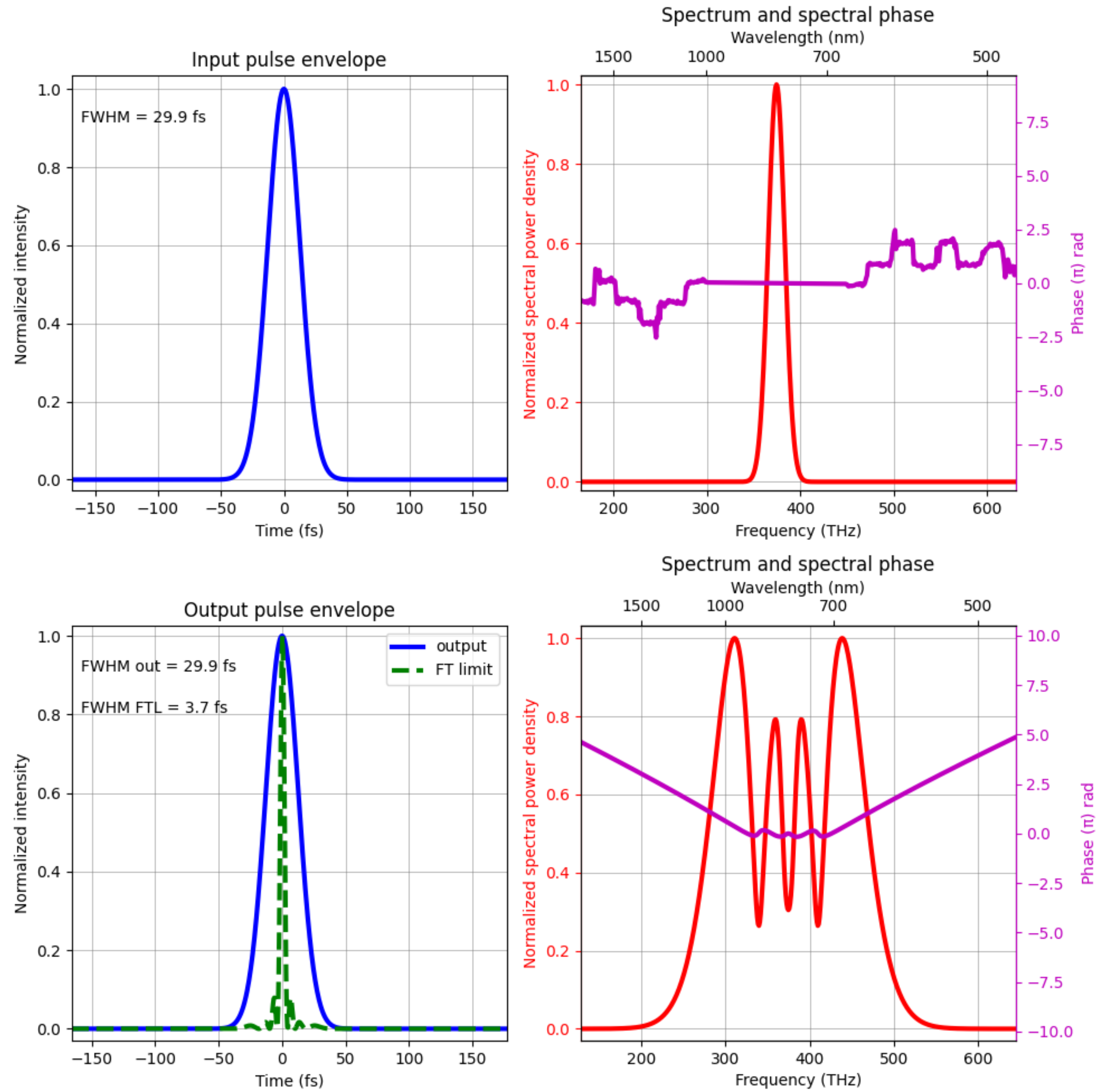

Self-steepening

Group velocity depends on pulse intensity

$$v_g = \frac{c}{n + \omega \frac{dn}{d\omega}}$$

$$n = n_o + n_2 I$$

Peak of the pulse gets delayed and generates a pulse asymmetry and spectral blue-shift

The shorter the pulse, the more important self-steepenging becomes

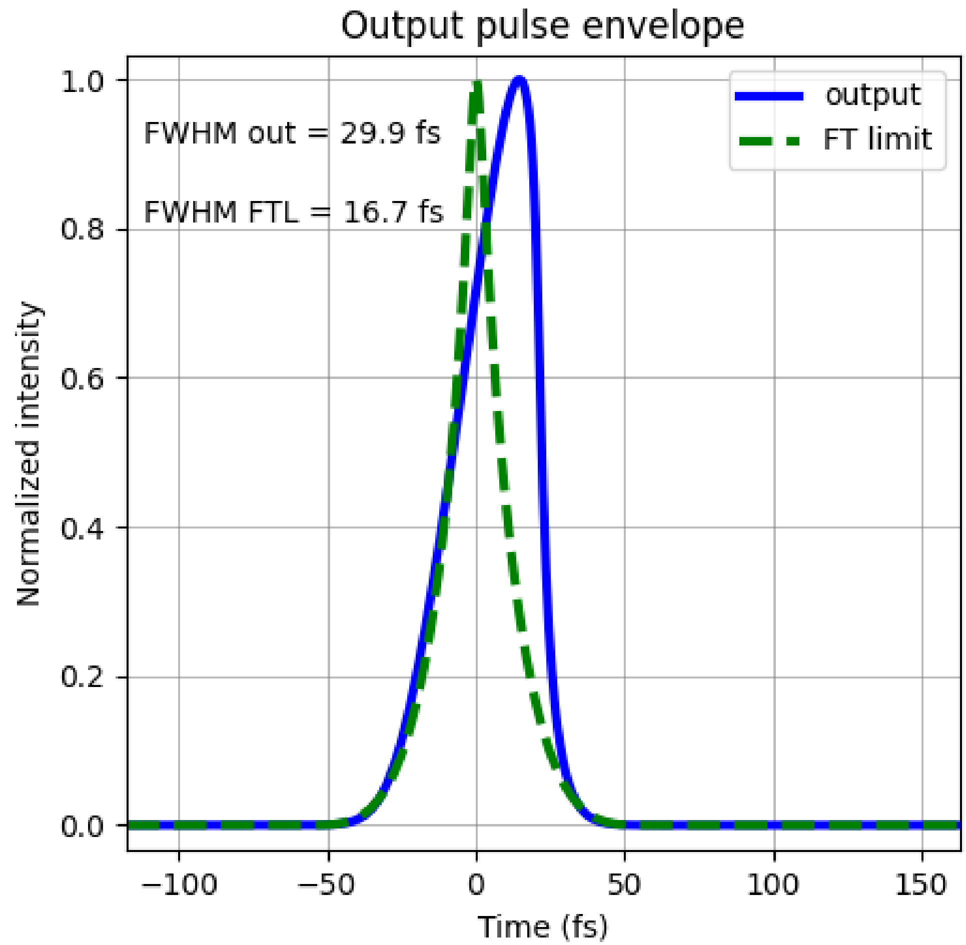

SPM + Self-steepening

$$\omega(t) = \frac{d\phi(t)}{dt} = \omega_0 - \frac{\omega_0}{c} n_2 z \frac{dI(t)}{dt}$$

- Leading edge of pulse contributes to new low frequencies, while the trailing edge creates new high frequencies

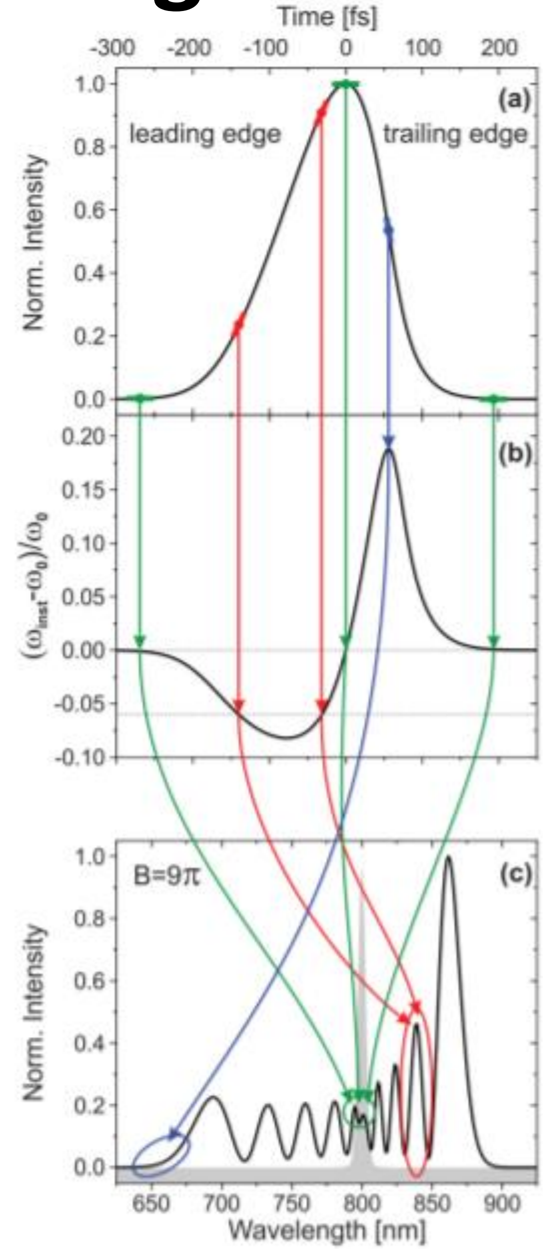

T. Nagy et al., Advances in Physics: X 6, 1845795 (2020)

SPM + Self-steepening

$$\omega(t) = \frac{d\phi(t)}{dt} = \omega_0 - \frac{\omega_0}{c} n_2 z \frac{dI(t)}{dt}$$

- Leading edge of pulse contributes to new low frequencies, while the trailing edge creates new high frequencies
- Always two points in time along the pulse with same slope: spectral modulation

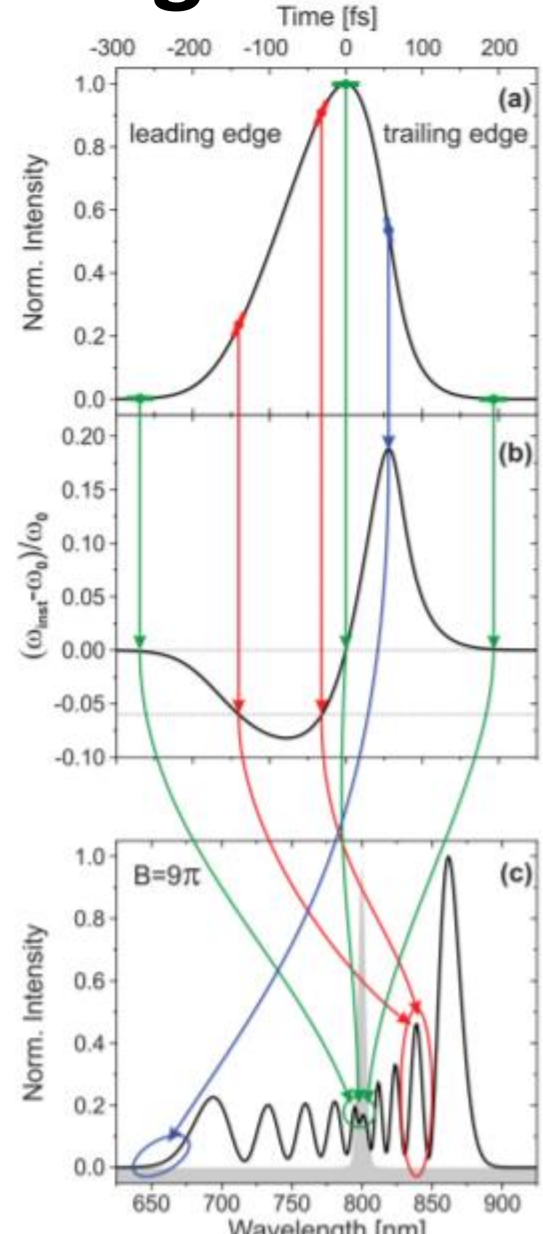

T. Nagy et al., Advances in Physics: X 6, 1845795 (2020)

SPM + Self-steepening

$$\omega(t) = \frac{d\phi(t)}{dt} = \omega_0 - \frac{\omega_0}{c} n_2 z \frac{dI(t)}{dt}$$

- Leading edge of pulse contributes to new low frequencies, while the trailing edge creates new high frequencies
- Always two points in time along the pulse with same slope: spectral modulation
- Around the peak and at the tails, the derivative is zero, so we have multiple contributions around the fundamental. Especially for pulses with several pedestals or satellites: fast oscillations around the fundamental

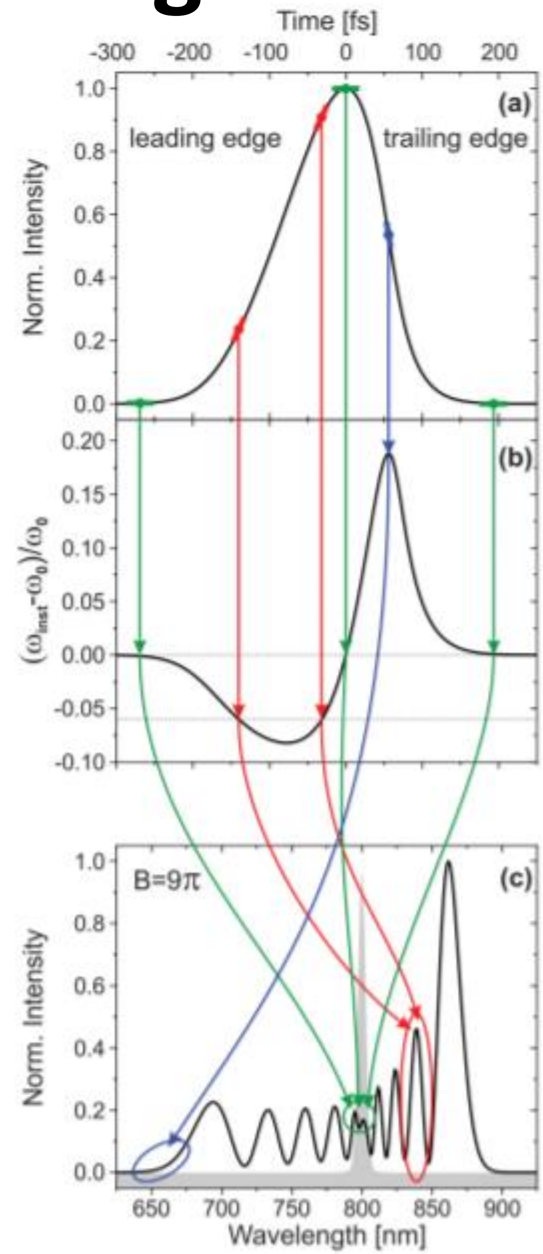

T. Nagy et al., Advances in Physics: X 6, 1845795 (2020)

Kerr effect: Self-focusing

$$\varepsilon = e^{i\frac{\omega_0 n_2}{c} I(x,y,t) z}, I(x,y) \propto e^{-2(x^2+y^2)/w^2}$$

- Spatially-dependent phase acts as a lens

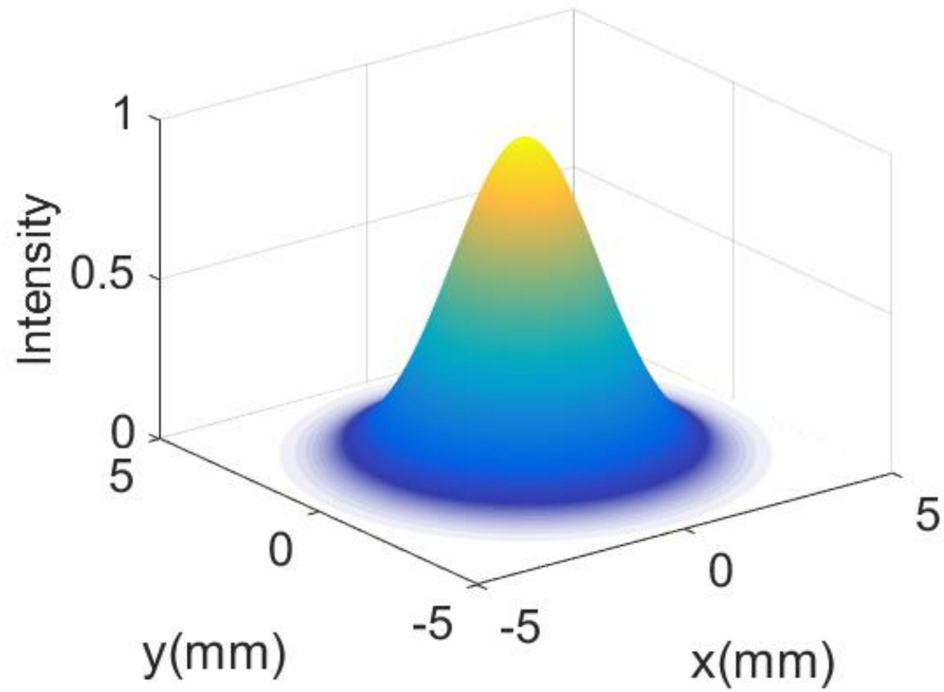

Kerr effect: Self-focusing

$$\varepsilon = e^{i\frac{\omega_0 n_2}{c} I(x,y,t) z}, I(x,y) \propto e^{-2(x^2+y^2)/w^2}$$

- Spatially-dependent phase acts as a lens
- With Gausian beams and paraxial approximation: wavefront curvature due to diffraction AND self-focusing depend on r^2

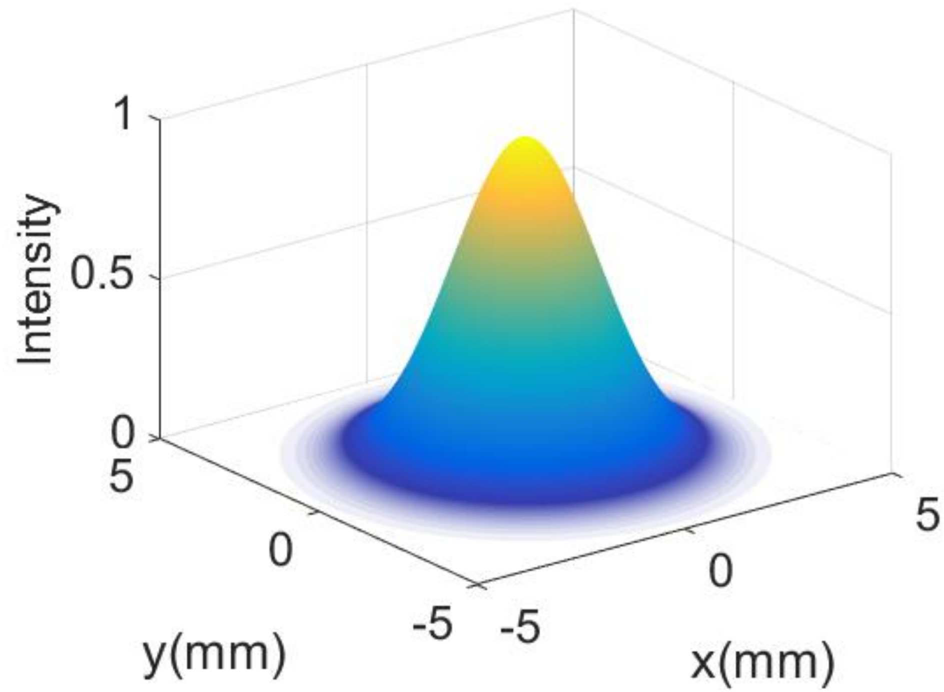

Kerr effect: Self-focusing

$$\varepsilon = e^{i\frac{\omega_0 n_2}{c} I(x,y,t) z}, I(x,y) \propto e^{-2(x^2+y^2)/w^2}$$

- Spatially-dependent phase acts as a lens
- With Gausian beams and paraxial approximation: wavefront curvature due to diffraction AND self-focusing depend on r^2
- $P_{cr} = \frac{3.72\lambda^2}{8\pi n_0 n_2}$ depends on peak power, not intensity!

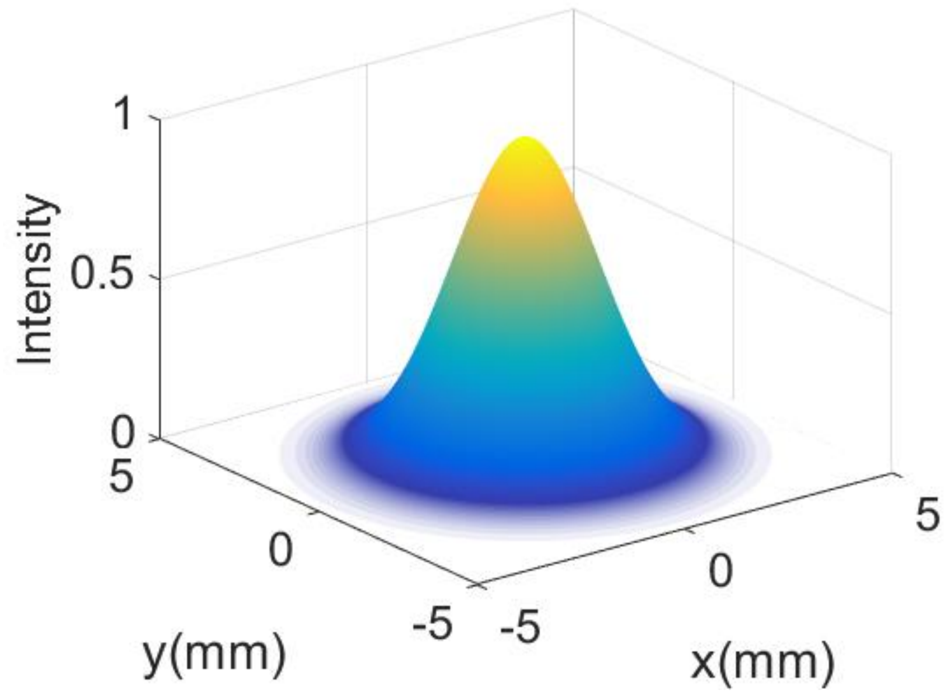

Kerr effect: Self-focusing

$$\varepsilon = e^{i\frac{\omega_0 n_2}{c} I(x,y,t) z}, I(x,y) \propto e^{-2(x^2+y^2)/w^2}$$

- Spatially-dependent phase acts as a lens
- With Gausian beams and paraxial approximation: wavefront curvature due to diffraction AND self-focusing depend on r^2
- $P_{cr} = \frac{3.72\lambda^2}{8\pi n_0 n_2}$ depends on peak power, not intensity!

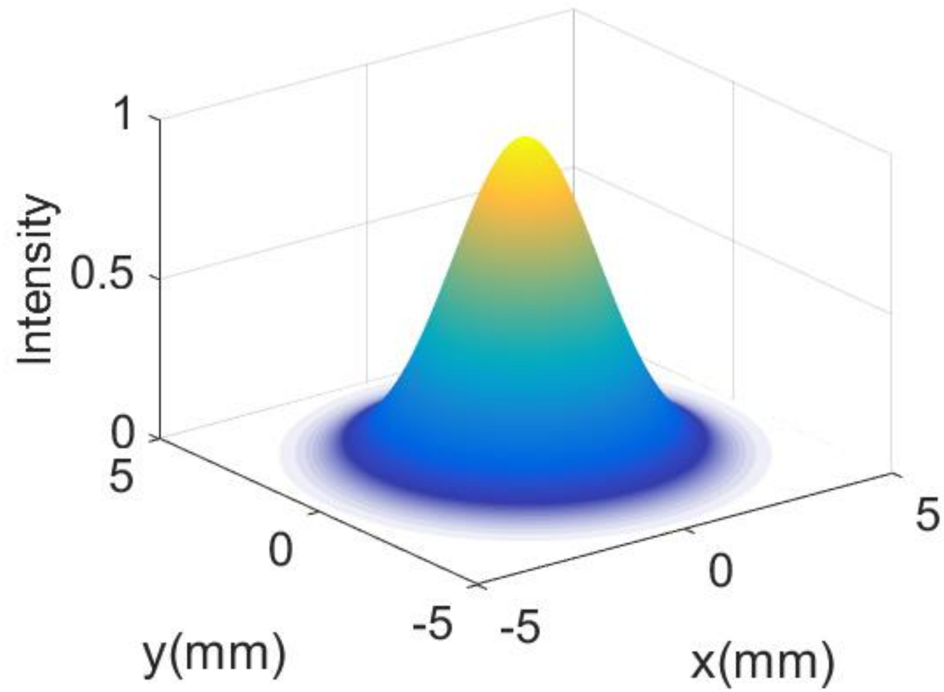

E = 0.5mJ, τ = 5fs, 800nm: P = 100GW

P_{cr_air} ≈ 2.2GW

Filamentation

- Self-focusing→colapse→ionization
- J becomes relevant
- Plasma defocusing
- Self-focusing+plasma defocusing = self-guiding (filament)

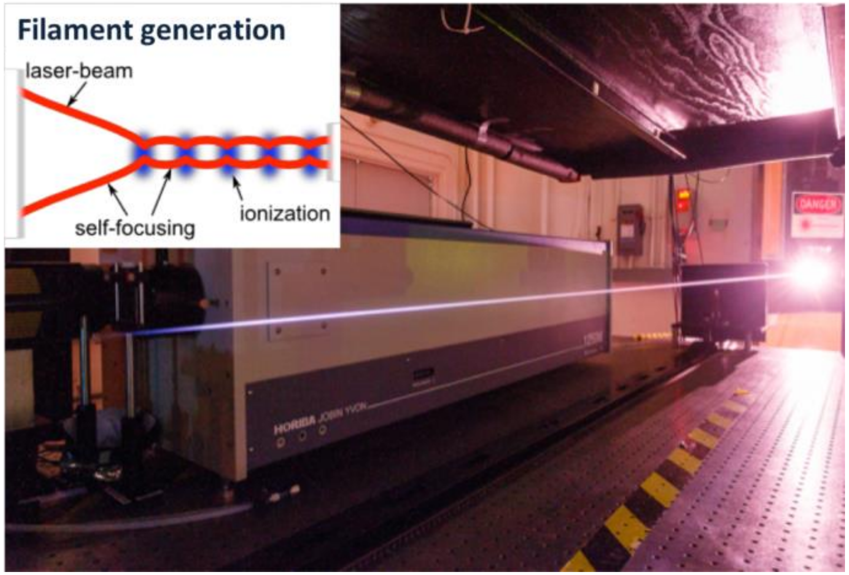

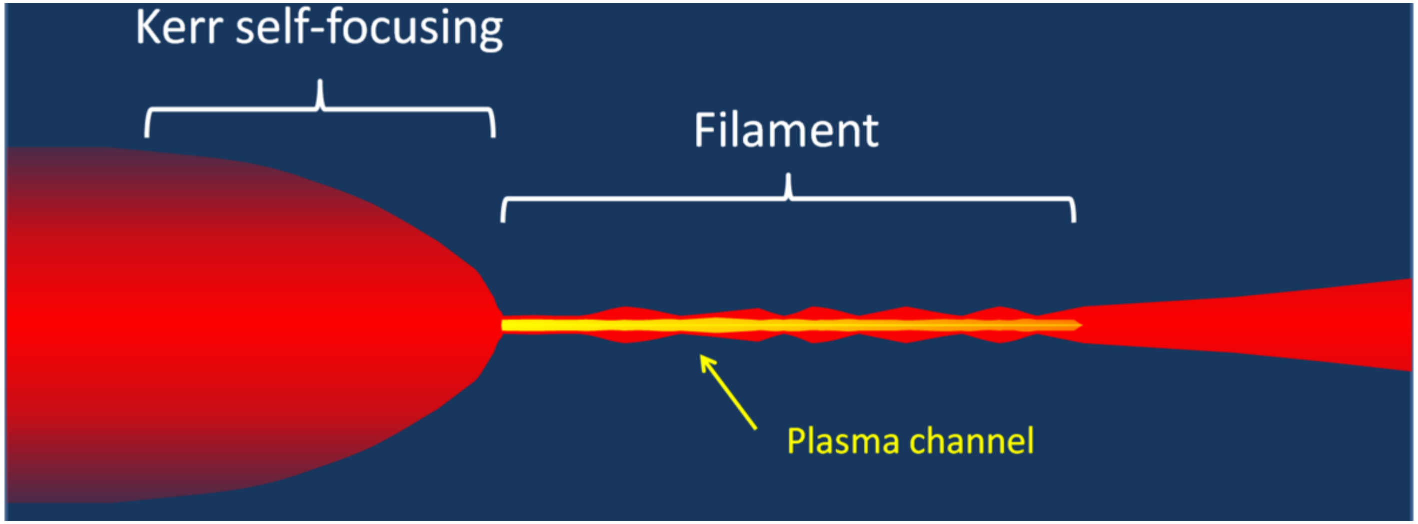

Images from https://laser-research.lbl.gov/research/remote/
and https://commons.wikimedia.org/wiki/File:Laser_filamentation

Examples

- Control/optimize spectral broadening with minimized self-focusing and space-time couplings
  - Hollow-fibers
  - Thin-plates
  - Multipass cells

Gas-filled hollow-core fibers

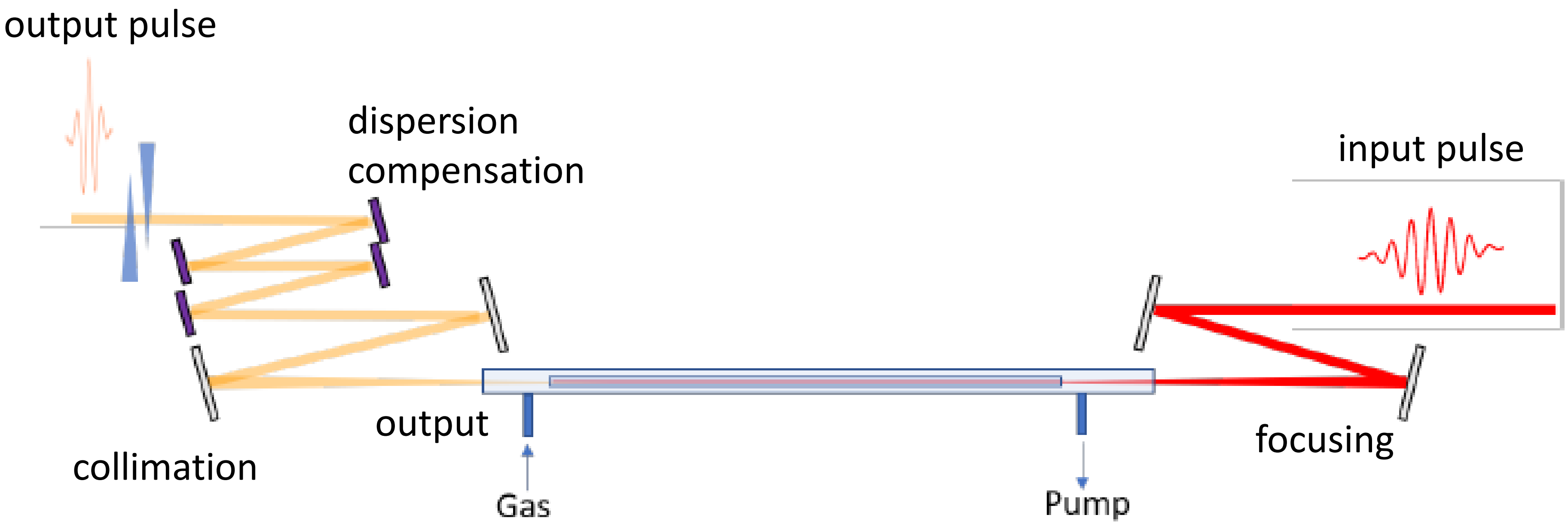

- Weak nonlinear interaction over long distances
- Mode confinement allows keeping high intensity beyond Rayleigh length
- Waveguiding ensures spatial mode quality
- Negligible space-time couplings

Nisoli et al., Opt. Lett. 22, 522-524 (1997)

Gas-filled hollow-core fibers

Optics Letters

Generation of above-terawatt 1.5-cycle visible pulses at 1 kHz by post-compression in a hollow fiber

Tamas Nagy,* Martin Kretschmar, Marc J. J. Vrakking, and Arnaud Rouzée

Highest peak power

Input puse: up to 14mJ, 50fs (800nm)
Output pulse: 6.1mJ, 3.8fs (~1.5 cycles)
HCF: 560μm diameter, 3.75m, He.

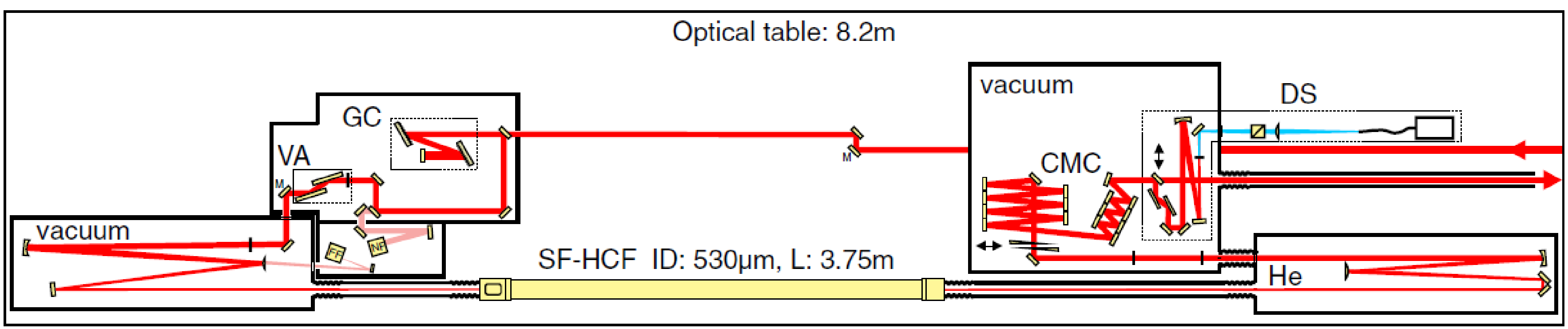

Gas-filled hollow-core fibers

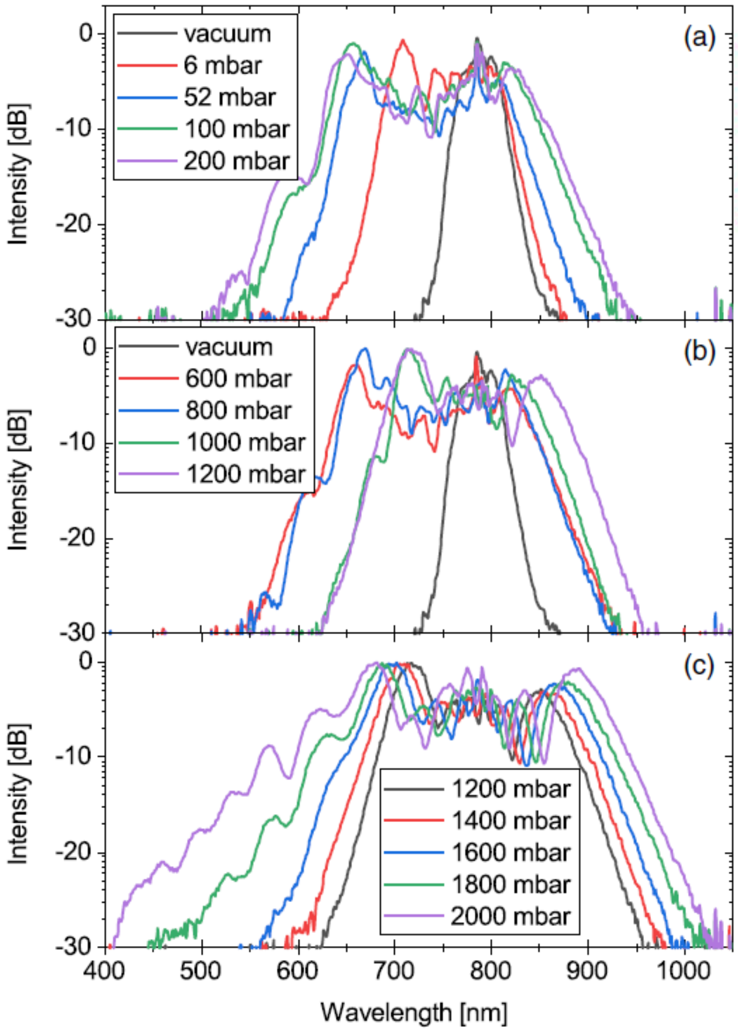

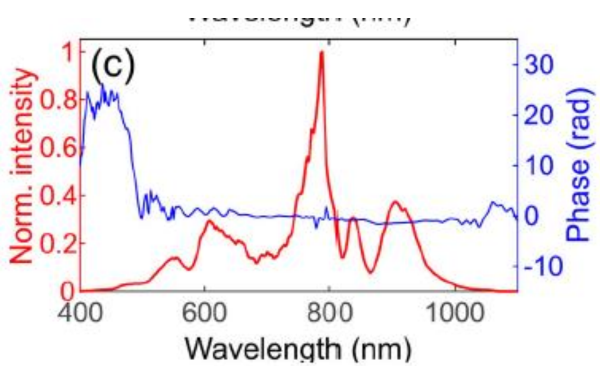

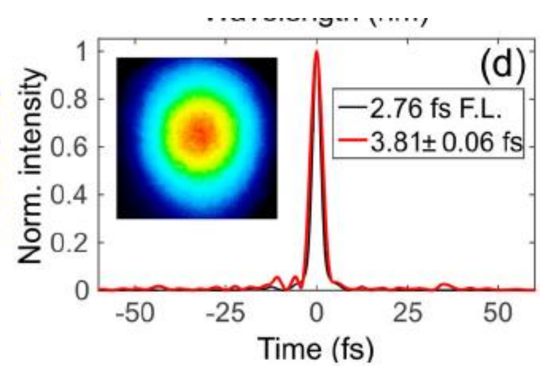

Input: 14mJ, 50fs (800nm) Ti:Sapp. CPA
output: 6.1mJ, 3.8fs (~1.5 cycles)
HCF: 560μm diameter, 3.75m, He.

Gas-filled hollow-core fibers

In: 7fs, <190μJ, 800nm, 100kHz from OPCPA. Out: <3.6fs, 95μJ,
HCF: 230μm core, 1m, Ne (2.5 bars)

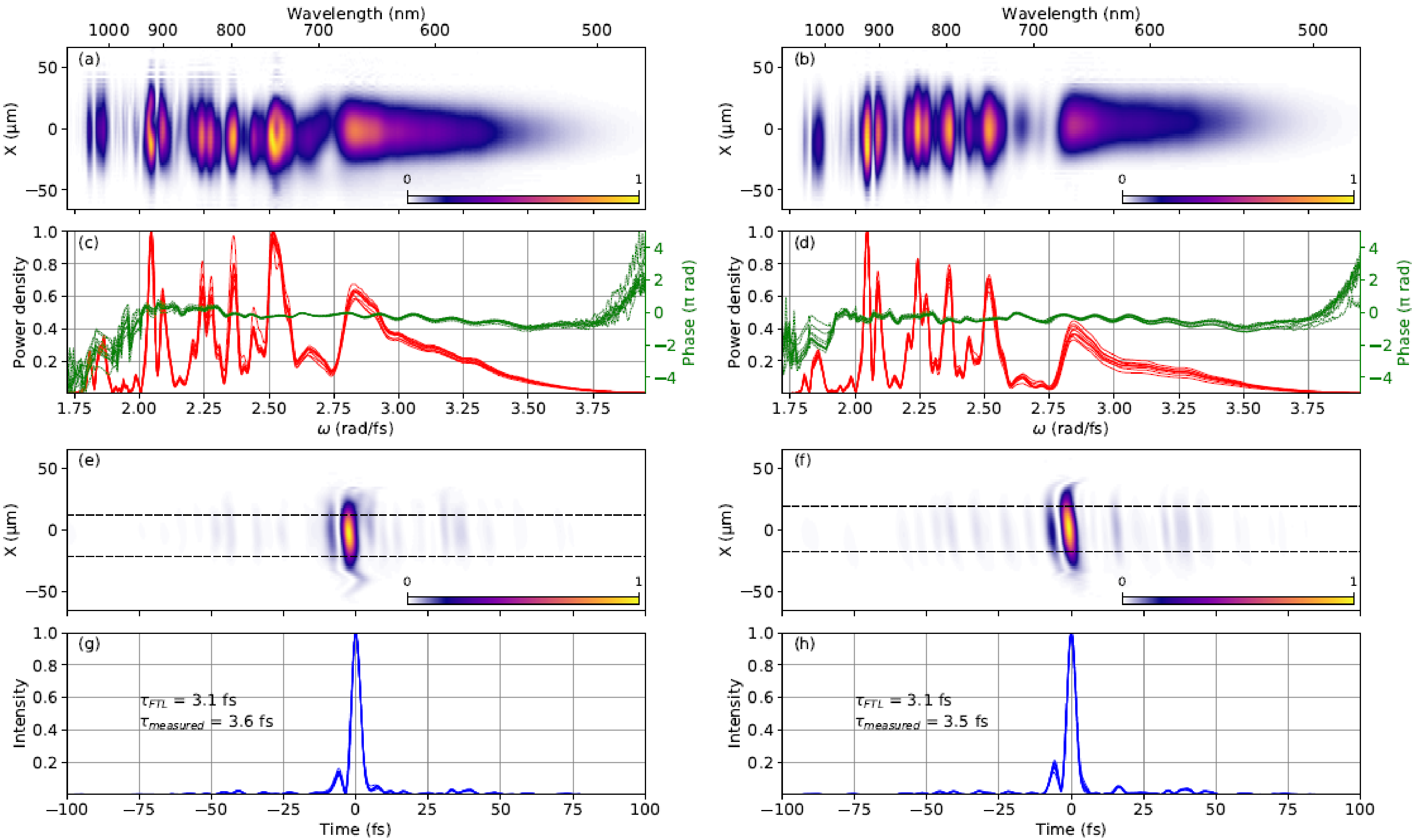

Furch et al., J. Phys. Photonics 4, 032001 (2022)

Multi-plate supercontinuum

sub-4fs from Ti:Sapp. CPA
con 0.2mJ, 1kHz, 25fs

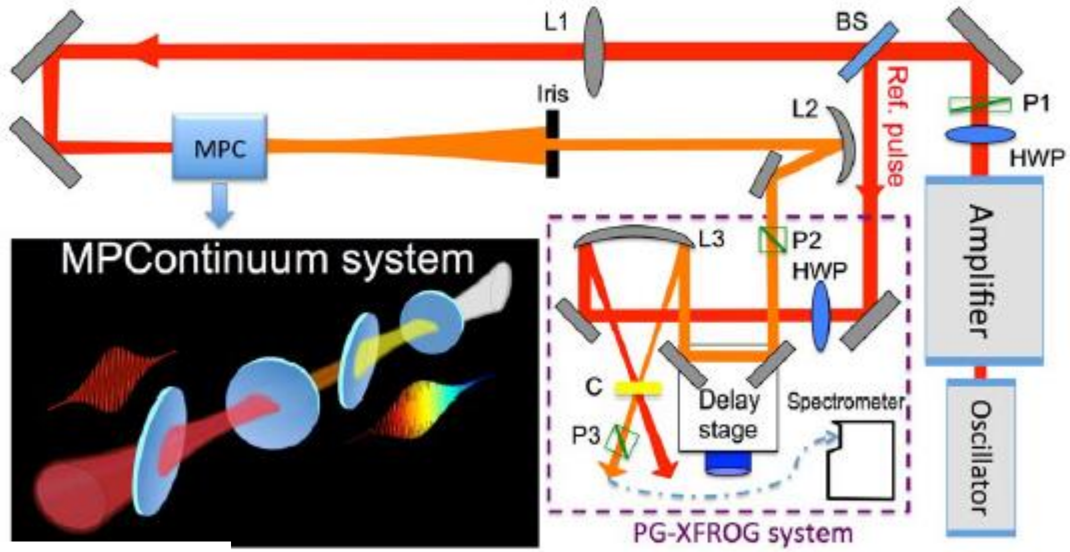

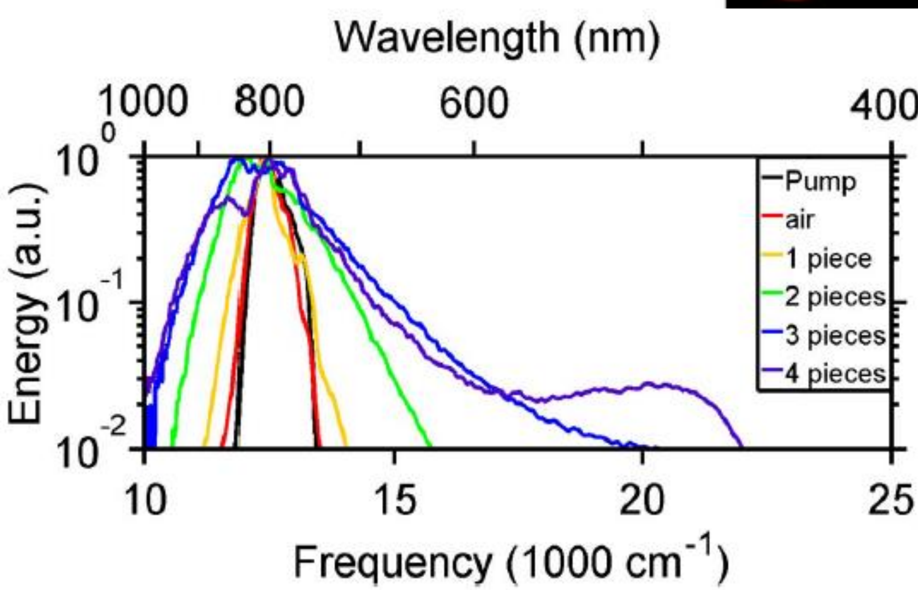

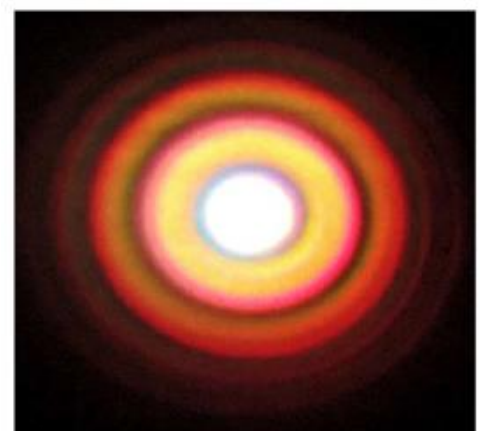

Lu et al., Optica 1, 400 (2014)

Multi-plate supercontinuum

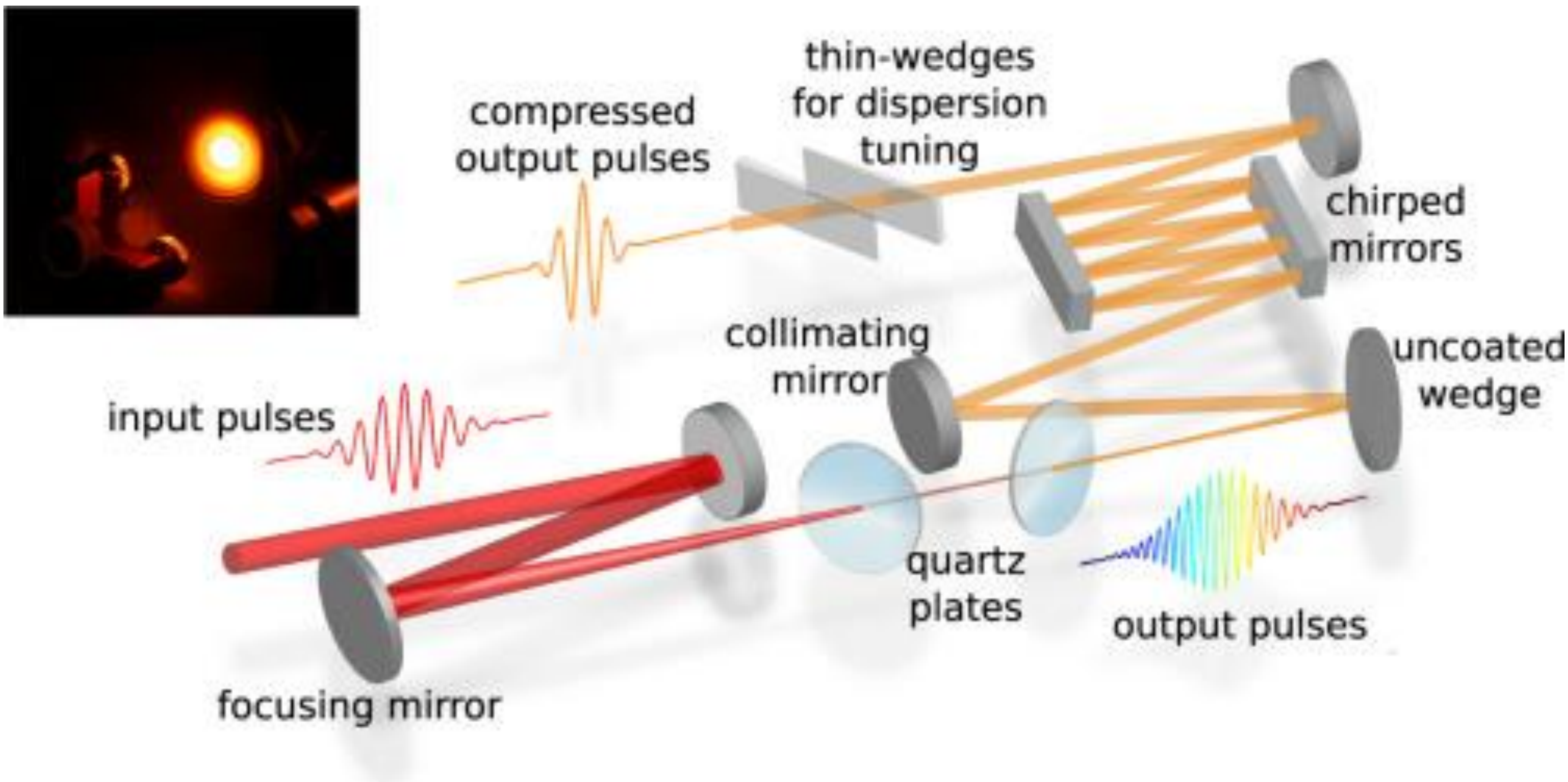

Lu et al., Opt. Exp. 26, 8941 (2018)

Multi-plate supercontinuum: sub-4 fs

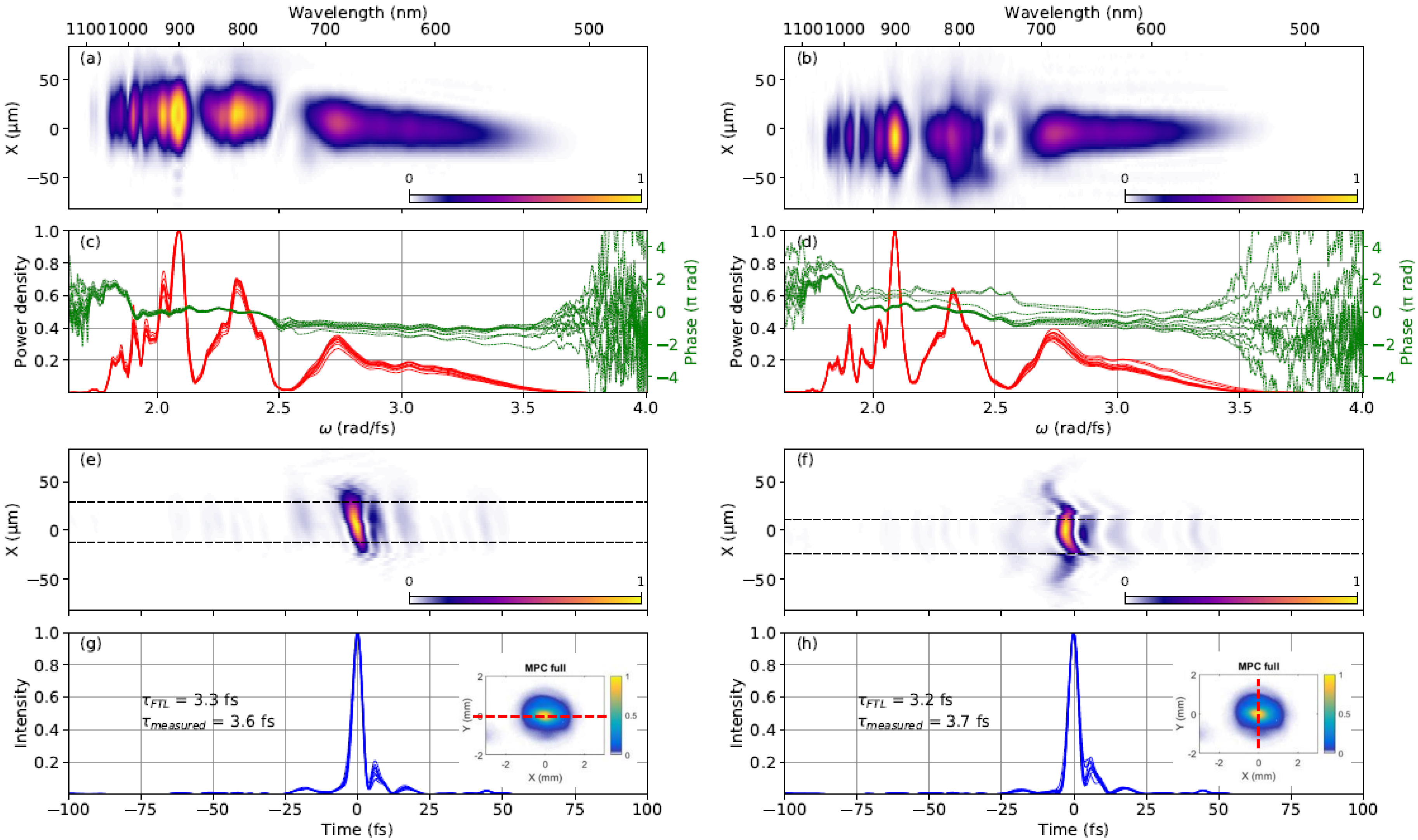

Data from Lu et al., Opt. Exp. 26, 8941 (2018)

Multipass cells

Off-Axis Paths in Spherical Mirror Interferometers

D. Herriott, H. Kogelnik, and R. Kompfner

April 1964 / Vol. 3, No. 4 / APPLIED OPTICS 523

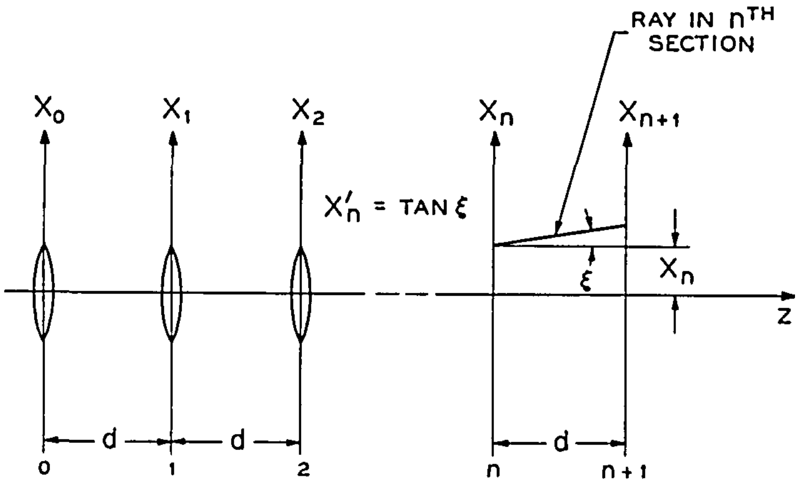

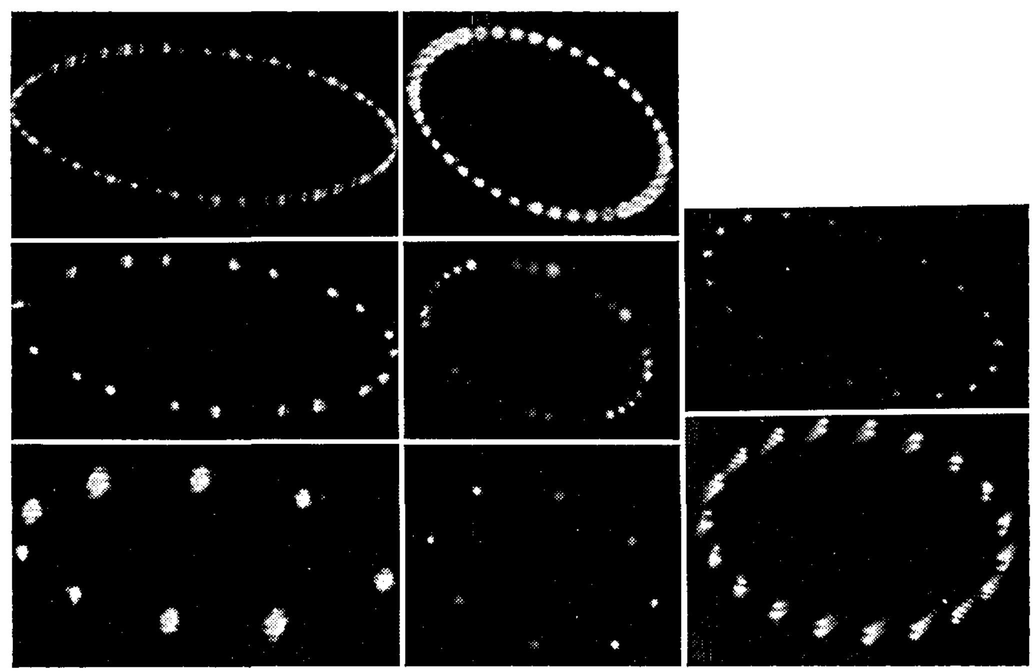

Multipass cells

Two-mirror multipass absorption cell

J. Altmann, R. Baumgart, and C. Weitkamp

15 March 1981 / Vol. 20, No. 6 / APPLIED OPTICS 995

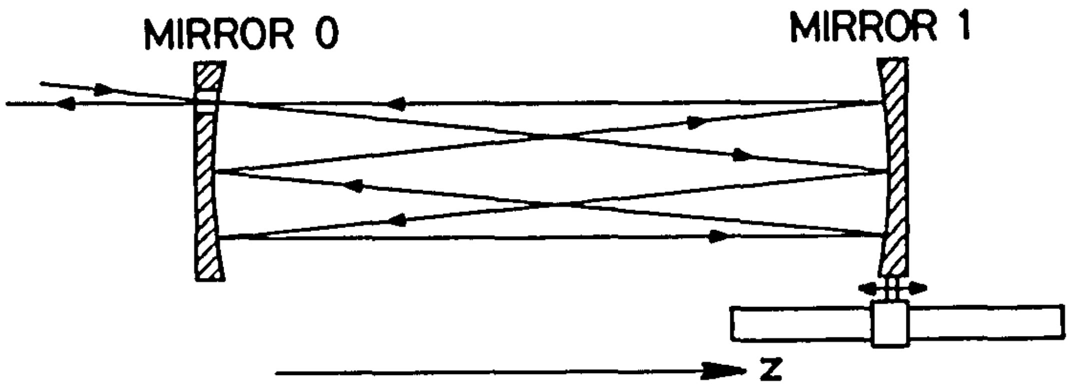

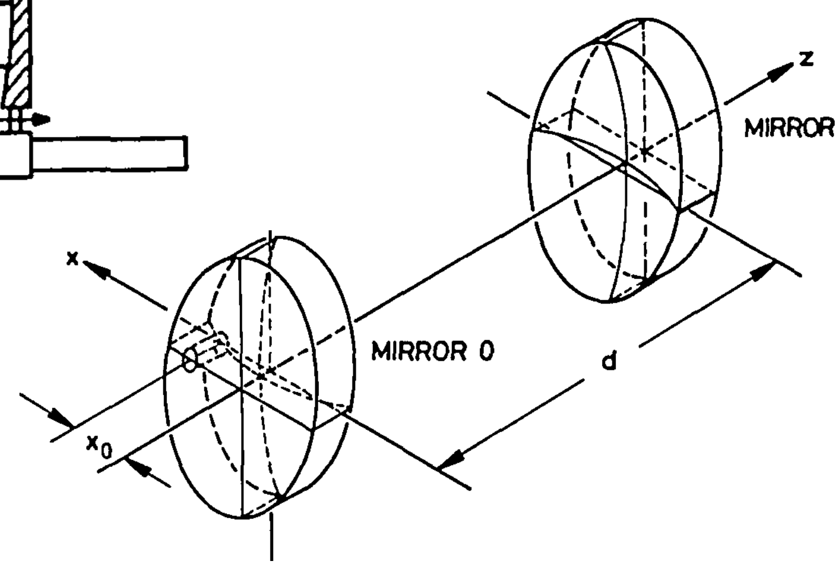

Multipass cells

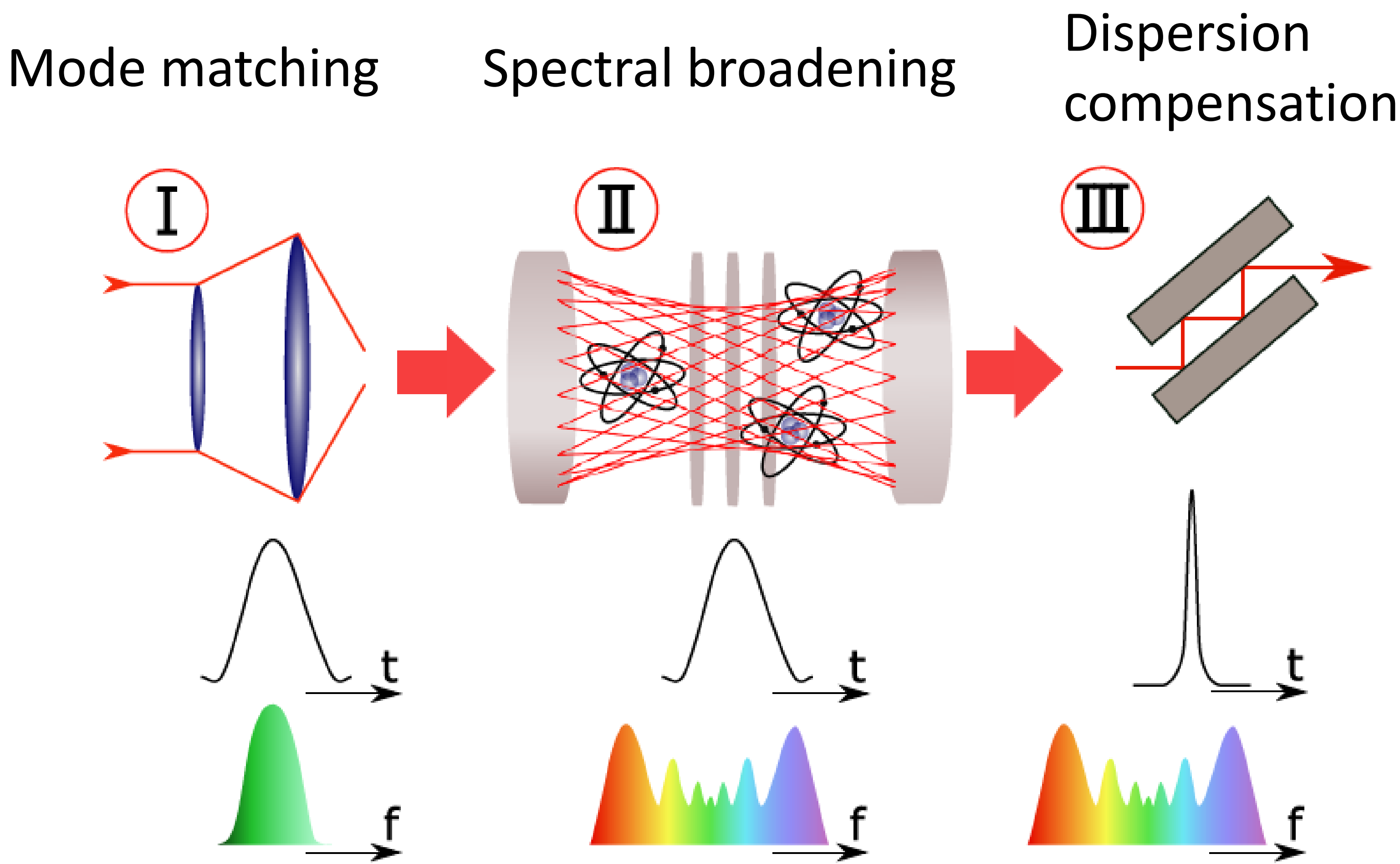

High-R mirrors → high efficiency (BUT not true for few-cycle pulses)

Image taken from Viotti et al., Optica 9, 197 (2022)

Post-compression: different methods

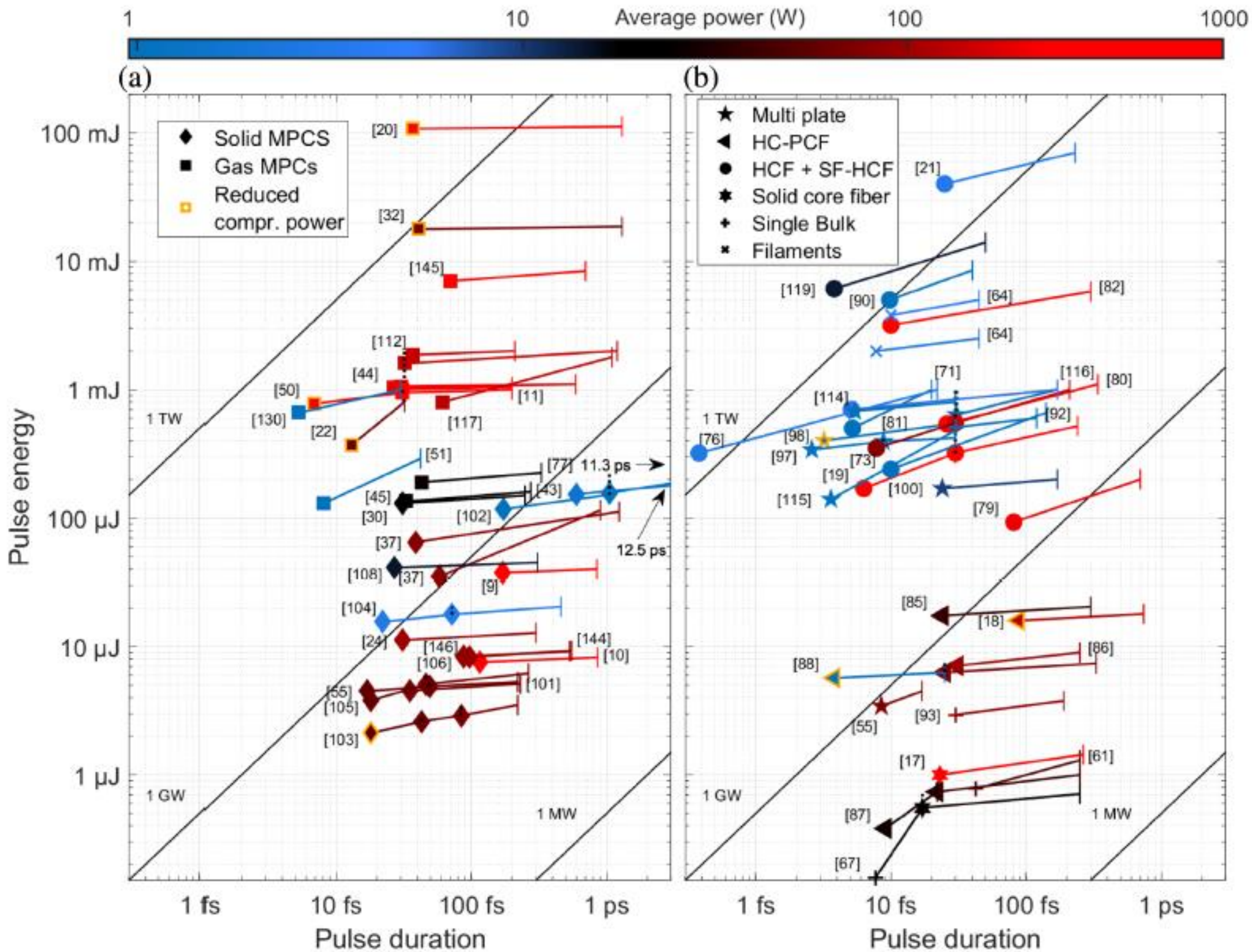

Image taken from Viotti et al., Optica 9, 197 (2022)

Multipass cells

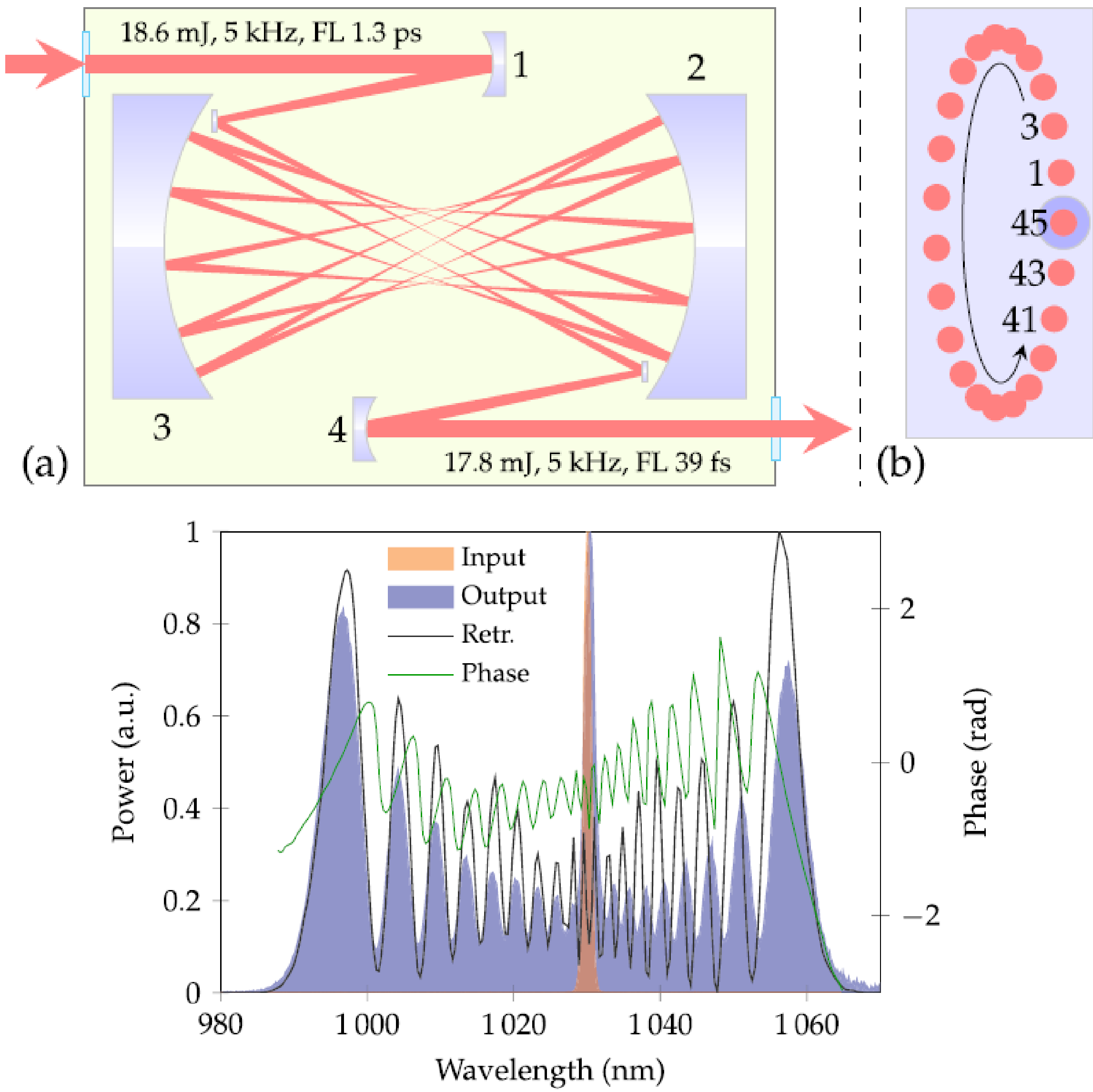

Kaumanns et al., Opt. Lett. 43, 5877 (2018)

Multipass cells

SHG-FROG measurement: 41 fs

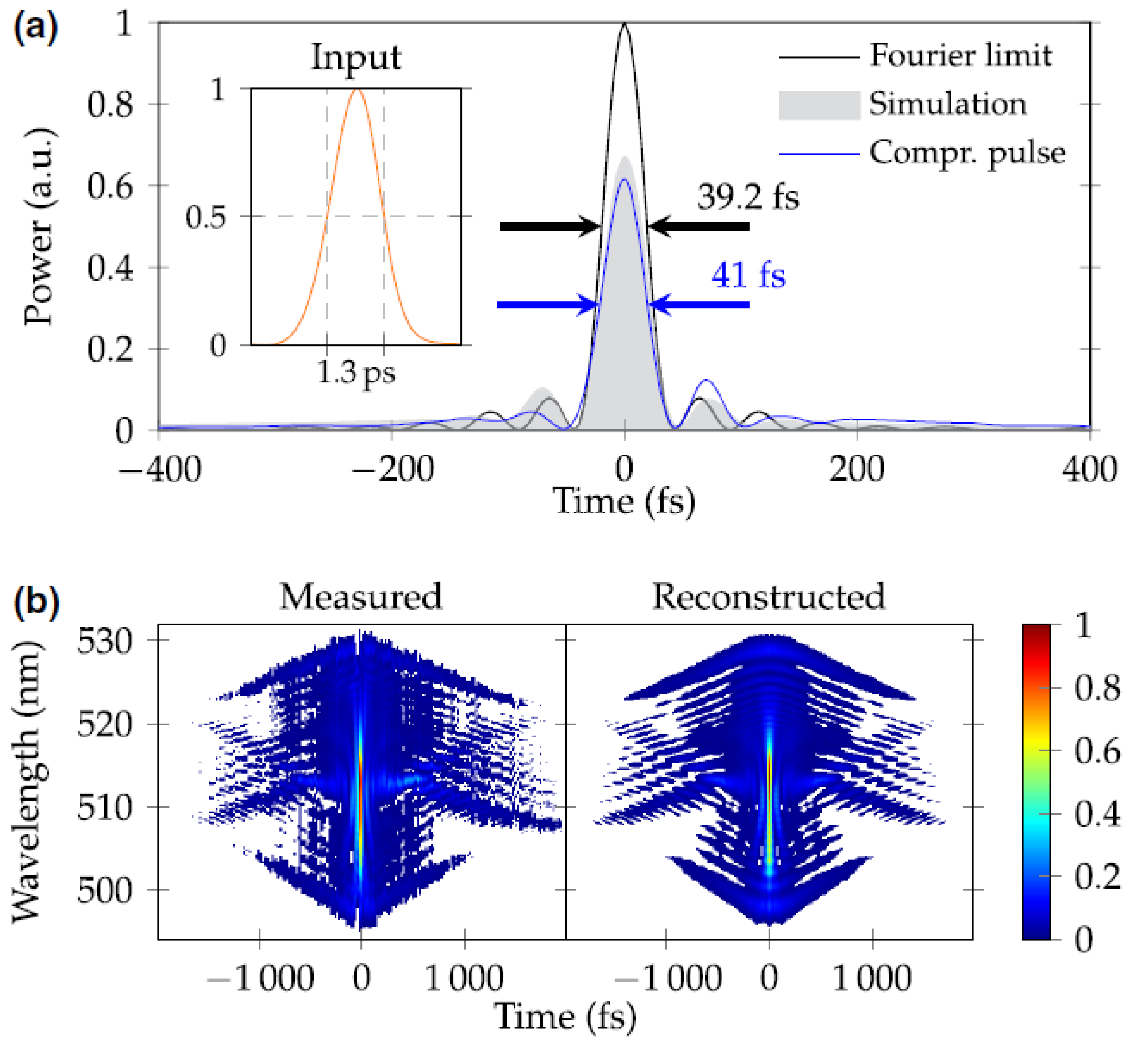

Kaumanns et al., Opt. Lett. 43, 5877 (2018)

Multipass cells

2678 Vol. 46, No. 11 / 1 June 2021 / *Optics Letters* **Letter**

Optics Letters

Multipass cell for high-power few-cycle compression

Michael Müller,[1,*] Joachim Buldt,[1] Henning Stark,[1] Christian Grebing,[1] Jens Limpert[1,2,3]

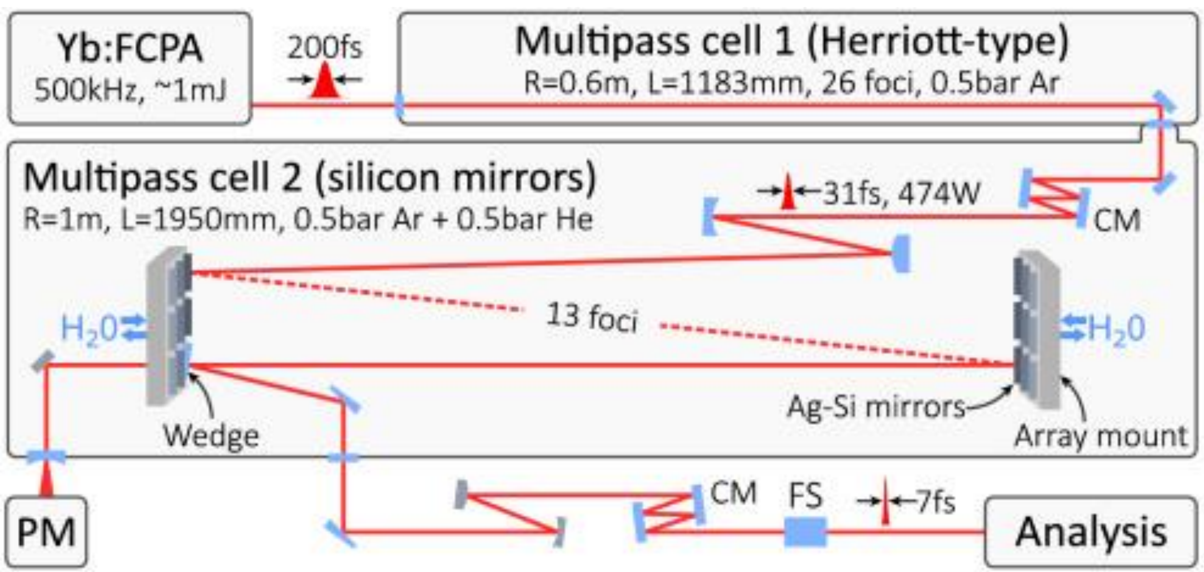

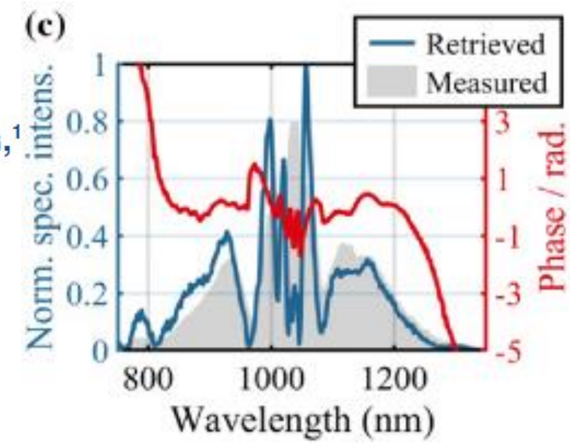

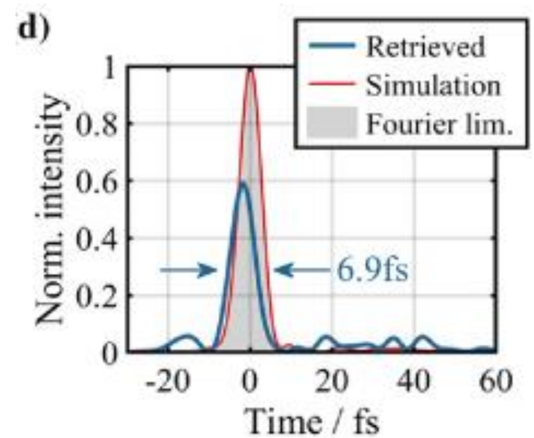

In: 200fs, ~1mJ, 500kHz (500W), 1030nm

Out: 6.9fs, 0.776mJ (η≈77%).

Comparison

- Control/optimize spectral broadening with minimized self-focusing and space-time couplings
  - Hollow-fibers: Excellent spatial and spatio-temporal properties. Easy to damage input of fiber.
  - Thin-plates: Simple to implement, impervious to pointing instabilities. Space-time couplings.
  - Multipass cells: high efficiency, impervious to beam pointing. Complexity increases and efficiency drops when reaching few-cycles.

Useful materials for further reading:

Couairon et al., “Practitioner’s guide to laser pulse propagation models and simulations,” Eur. Phys. Journal **199**, 5-76 (2011).

M. Hanna et al., “Nonlinear temporal compression in multipass cells: theory, ” JOSA B 34, 1340 (2017)

Jan Schulte, et al., "Nonlinear pulse compression in a multi-pass cell," Opt. Lett. 41, 4511-4514 (2016)

Viotti et al., Optica 9, 197 (2022)

Lu et al., Optica 1, 400 (2014)

T. Nagy et al., Advances in Physics: X 6, 1845795 (2020)